Seminar series nr 221

Assessing vegetation changes for parts of the Sudan and Chad during 2000-2010 using time series analysis of MODIS-NDVI

Salem Beyene Ghezahai

2011
Department of Earth and Ecosystem Sciences
Physical Geography and Ecosystems Analysis
Lund University
Sölvegatan 12
S-223 62 Lund
Sweden

Salem Beyene Ghezahai (2011). Assessing vegetation changes for parts of the Sudan and Chad during 2000-2010 using time series analysis of MODIS-NDVI
Master degree thesis, seminar series 221, 30 credits in Geomatics
Department of Earth and Ecosystem Sciences, Physical Geography and Ecosystems Analysis, Lund University

Assessing vegetation changes for parts of the Sudan and Chad during 2000-2010 using time series analysis of MODIS-NDVI

Salem Beyene Ghezahai 2011

Master degree thesis in the Division of Physical Geography and Ecosystems Analysis, Department of Earth and Ecosystem Sciences

Supervisor
Jonas Ardö (Ph.D)
Division of Physical Geography and Ecosystems Analysis
Department of Earth and Ecosystem Sciences
Lund University

Abstract

Phenological vegetation characteristics are valuable inputs to several ecosystem-related models: including carbon exchange and climate change. Phenological characteristics are effective measures of changes in vegetation in an area and are subject to the seasonal and inter-annual climatic variations. In arid and semi-arid ecosystems, precipitation is the main driving factor for changes in vegetation and phenological parameters. In this regard, remotely sensed vegetation indices are widely used. In the current study, time series of 16-day composite normalized difference vegetation index (NDVI) images from Moderate Resolution Imaging Spectroradiometer (MODIS) were analyzed to assess vegetation changes for parts of the Sudan and Chad (between 10^{o}-20^{o} Northern latitude and 23^{o}-35^{o} Eastern longitude) during 2000-2010. Spatial and temporal variation in NDVI and phenological (seasonality) parameters were assessed for the land cover classes shrubland, grassland, cropland and savanna. Mathematical models from TIMESAT, a program package developed for extracting seasonality parameters from a series of data captured using remote sensing techniques over time, were implemented to suppress the noisy patterns in NDVI and to extract phenological parameters. The observed changes were then explained by looking at the amount of rainfall. Even though the results cannot be generalized, majority of the cases depict an increase in the fitted NDVI, delay on the start and end of the growing seasons, shortening of growing season length, decrease in amplitude and integrals. However, statistical test outputs were not significant for most of the cases. This could be due to the effect of small sample sizes, which increase the likelihood of obtaining erroneous results and further inspection is recommended. In general, high temporal and spatial variations were evident. The temporal variation could mainly be attributed to the erratic nature of the rainfall. The spatial variation is also a factor of the strong north-south rainfall diversity. Even so, the results depict that rainfall amount only cannot explain the observed changes.

Keywords: Geography, Physical Geography, NDVI, MODIS, TIMESAT, time series, land cover, temporal variation, spatial variation, rainfall, phenological parameters, vegetation

Acknowledgements

I would like to extend my deep, sincere gratitude to my supervisor Jonas Ardö (Ph.D) for the inspiration, guidance and support throughout the project. I would also like to acknowledge and extend my heartfelt appreciation to the following individuals and organizations, who made the completion of this dissertation possible.

Lars Eklundh (Ph.D) from Lund University and Per Jönsson (Ph.D) from Malmö University, for granting the access to TIMESAT. Particularly, Lars Eklundh for the technical guidance and support throughout.

Earth Observing System Data and Information System (EOSDIS) 2009, Earth Observing System ClearingHOuse (ECHO) / Warehouse Inventory Search Tool (WIST) Version 10.X, Greenbelt, MD: EOSDIS, Goddard Space Flight Center (GSFC) National Aeronautics and Space Administration (NASA) (URL: https://wist.echo.nasa.gov/api/), for providing MODIS data used in this study. These data are distributed by the Land Processes Distributed Active Archive Center (LP DAAC), located at the U.S. Geological Survey (USGS) Earth Resources Observation and Science (EROS) Center (lpdaac.usgs.gov).

Famine Early Warning System Network (FEWS NET), climate prediction center (CPC/Famine Early Warning System Daily Estimates) for providing rainfall data.

Erasmus Mundus External Cooperation Window-Lot10 (EMECW-Lot10) coordinated by Petter Pilesjö, for financial support during my study period.

All faculty members and Staff of the Department of Earth and Ecosystem Sciences, Division of Physical Geography and Ecosystems Analysis, Lund University, Sweden for the remarkable stimulus, hospitable and understanding quality.

My colleagues at the Division of Physical Geography and Ecosystems Analysis, for their valuable discussion and knowledge-sharing behaviors, particularly Eduard Mikayelyan for technical assistance.

Most especially to my family and friends, for their endless encouragement, enthusiasm, motive and aspirations.

And above all to the Almighty God, for giving me the strength and health throughout and made all things possible.

Dedication

This thesis work is dedicated to my parents for their unending love, for everything they gave me throughout my life and always being there for me.

And

specially to my father, whom I lost few weeks before I finalize my study.

Table of Contents

List of tables and figures

List of tables

List of figures

Acronyms and Abbreviations

amsl.	above mean sea level
AMSU	Advanced Microwave Sounding Unit
AVHRR	Advanced Very High Resolution Radiometer
BRDF	Bi-directional Reflectance Distribution Function
CPC	Climate Prediction Center
DN	Digital Number
ECHO	Earth Observing System Clearing House
EOS	Earth Observing Systems
HDF-EOS	Hierarchical Data Format - Earth Observing System
fAPAR	Fraction of Absorbed Photosynthetically Active Radiation
FEWS	Famine Early Warning System
GOES	Geostationary Operational Environmental Satellite
GPI	GOES Precipitation Index
GPP	Gross Primary Production
GTS	Global Telecommunication Stations
IGBP	International Geosphere-Biosphere Program
ITCZ	Inter-Tropical Convergence Zone
JISAO	Joint Institute for the Study of the Atmosphere and Ocean
LAI	Leaf Area Index
LC	Land cover
LUE	Light Use Efficiency
LWIR	Long Wavelength infrared
MWIR	Middle Wavelength infrared
MERIS	Medium Resolution Imaging Spectrometer
mm.	millimeter
MODIS	Moderate Resolution Imaging Spectroradiometer
MSG	Meteostat Second Generation
NDVI	Normalized Difference Vegetation Index
NearIR	Near Infrared
nm.	nanometer
NOAA	National Oceanic and Atmospheric Administration
NPP	Net Primary Productivity
SSM/I	Special Sensor Microwave/Imager
SPOT	Système Pour l'Observation de la Terre
SST	Sea Surface Temperature
SWIR	Short Wavelength infrared
UNEP	United Nations Environment Program
UNSO	United Nations Sudano-Sahelian Office
VI	Vegetation indices/index
WIST	Warehouse Inventory Search Tool

Definition of terms

Arid: a region with permanent scarcity of precipitation. It is also characterized by high temperature, high evapo-transpiration and low humidity.

BRDF: refers to reflected light as a function of viewing and sun angle during off-nadir view leading to variable reflectance from the same target.

Drought: refers to a temporary situation related to decreased precipitation amount, in relation to the normal amount observed in a particular area.

Electromagnetic spectrum: is a range of wavelengths in which objects on the surface radiate electromagnetic waves.

ITCZ: a rising air mass near the equator. It shifts in the north-south direction seasonally and produces cloudiness and heavy rainfall.

Lambertian surface: an ideal and perfectly diffusing surface, in which incident energy is equally reflected in all the directions.

Land cover: refers to the physical and biological cover over land surface, including water, vegetation, bare soil, and/or artificial structures.

Land degradation: refers to the change observed in the physical, chemical and/or biological properties of the soil affecting its productive potential.

Nadir: a point on the surface directly below a sensor.

Noise: refers to a disturbance or unwanted signal.

Path length: the distance energy must travel through the atmosphere.

Smoothing: a noise reduction technique using different model functions, whereby variations of short frequency are suppressed.

Spatial variation: refers to variation observed at different locations.

Sun angle: refers to the position of the sun relative to the earth.

Temporal variation: refers to variation observed over time.

Vegetation phenology: is the study of seasonal timing in vegetation growth in response to environmental factors such as rainfall and temperature.

Vegetative condition: refers to the growth stage of plants in which photosynthetic activity starts.

Time series: refers to a set of observations, results, or other datasets obtained over a period of time, usually at regular intervals.

Spectral property: refers to the characteristic of an object measured within a specific wavelength interval.

1. Introduction

1.1. Background

Environmental monitoring requires the quantification of the parameters that control the biophysical processes and energy exchanges (Townshend et al., 1991). Vegetation plays a fundamental role in the physiographic setting of an area. Changes in vegetation have profound impacts on the global environment including ecosystem functions and the climate (Townshend et al., 1991; Salim et al., 2008). Besides, land use / land cover changes play an important role in climate change through alterations in the local evapo-transpiration, which affects the water cycle, atmosphere-vegetation interactions and greenhouse gas emissions (Eltahir 1996; Canadell and Noble, 2001).

Knowledge of the global vegetation distribution is, hence, crucial for understanding different ecosystem processes and the process of the earth's system as a whole (Jones et al., 1998; Fensholt, 2004). The ecosystem processes include: terrestrial primary productivity, hydrologic cycle and surface-atmosphere energy transfer (Tucker et al., 1985; Townshend et al., 1991). These processes are responsive to changes in climate and solar radiation, which is the main source of energy for maintaining the structure and function of the ecosystem (Monteith, 1972). Similarly, the radiative property of the surface of the earth is determined by land cover conditions, topography, albedo and other physical variables. These variables influence the flux of energy, carbon dioxide and other greenhouse gases between the earth and the atmosphere and consequently the global climate (Strahler et al., 1999; Zhan et al., 2002).

However, vegetation is under constant alteration due to climatic effects and / or human activities in the struggle for survival including afforestation (Hickler et al., 2005; Katagis et al., 2006). Explicitly, biomass production and removal for consumption is one of the causes; since vegetation net primary productivity (NPP) is the source of food supply for humans, fodder for herds and wood for construction and fuel (Seaquist, 2001; Héllden and Tottrup, 2008).

Modelling terrestrial ecosystem, carbon exchange and climate change require the knowledge of phenological vegetation characteristics. Phenology (derived from Greek words phaino meaning to bring light and logos meaning study) is the study of periodic plant and animal life cycle events and the influence of seasonal and inter-annual climate variations (Eklundh and Jönsson, 2009; wikipedia.org/wiki/Phenology). These characteristics are influenced by seasonal and inter-annual climatic variations and are effective measures of changes in vegetation of an area (Zhang et al., 2005). In arid and semi-arid ecosystems, precipitation is the main factor controlling phenology of plants. Global climate change is another, due to its influence on the seasonality of rainfall and extreme weather events: such as floods and droughts (Zhang et al., 2005; Héllden and Tottrup, 2008).

Using remote sensing technologies the spectral, temporal, spatial and directional information of different objects on the earth's surface could be acquired. In other words, the reflectance as a function of wavelength, time, location and sensor view angle, respectively, could be captured (Strahler et al., 1999; Hyman and Barnsley, 1997). From remotely sensed data, an insight of the global vegetation distribution, their inherent biophysical and structural properties, as well as the temporal and spatial disparity could be obtained (Huete et al., 1999). Leaf area index (LAI), fraction of absorbed photosynthetically active radiation (fAPAR),

percent green cover, biomass and net primary productivity (NPP) refer to the biophysical vegetation properties while canopy structure and orientation are part of the structural properties (Huete et al., 1999).

Launched first in 1978, the Advanced Very High Resolution Radiometer (AVHRR) satellite sensor provides long time series of data with global coverage for qualitative and quantitative assessment of environmental aspects (Defries et al., 2000; Fensholt & Sandholt, 2005). Qualitative environmental studies deal with the assessment of changes in land cover while the quantitative aspects deal with the biophysical parameters that take part in the environmental processes (Defries et al., 2000). Other satellite sensors (such as MODIS and MERIS) launched in the late 1990's; provide data for environmental monitoring studies with improved radiometric and spatial resolutions (Fensholt & Sandholt, 2005).

To ensure consistent and reliable monitoring of the terrestrial ecosystem, the vegetation spectral responses measured using Earth Observing Systems (EOS) is enhanced to a reflected vegetation signal by combining different bands (Huete et al., 1999). The observation of the surface conditions is made using the spectral properties of vegetation, most commonly vegetation indices (VI), since these indices are correlated to many biophysical variables (Huete et al., 1999; Zhang et al., 2003). For instance, the normalized difference vegetation index (NDVI) has largely been applied in several vegetation studies as it is correlated to NPP, LAI, green biomass, percent green cover and fAPAR (Goward et al., 1991; Huete et al., 1999; Zhang et al., 2003; Olsson et al., 2005; Katagis et al., 2006). Moreover, NDVI is used as input to several models related to nutrient cycle since it is related to carbon fixation, canopy resistance and potential evapo-transpiration (Huete et al., 1999).

1.1.1. The Sahel

The Sahel is a biogeographic zone bounded by the Sahara desert in the north and Sudanian savanna in the south. It extends between the Atlantic Ocean to the west and the Red Sea to the east (Houerou 1980). Figure 1.1, adapted from Fensholt et al., (2009), shows an overview of the Sahel region.

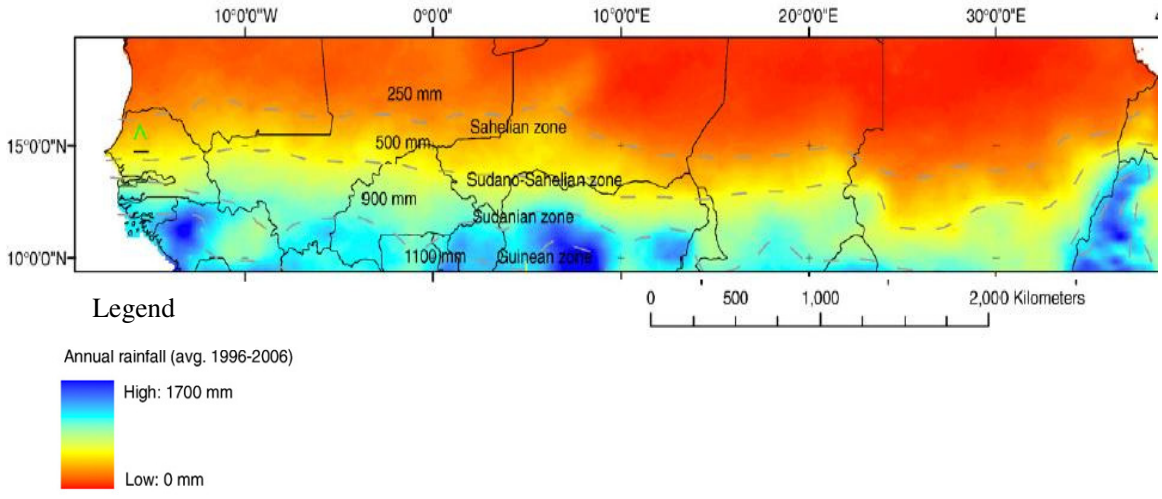

Figure 1.1: Overview map of the Sahel

The Sahel is a dynamic environment responding to both changes in climate and human activities (Herrmann et al., 2005; Olsson, 2008). This region is also highly responsive to sea surface temperature (SST) variations in the Pacific, Atlantic and Indian Oceans in the tropics (Giannini et al., 2003). It is characterized by arid climate with a mean annual precipitation between 100 and 600 mm (Seaquist, 2001). Northward movement of moist air masses and their interaction with Inter-Tropical Convergence Zone (ITCZ) drives the rainy season in this region. The rainy season lasts approximately between May and October (Houerou, 1980; Prince et. al., 1995) and maximum is commonly observed in August (Justice and Hiernaux, 1986). High spatial and temporal rainfall variability is observed in the north-south direction (Marseli, 1992; Prince et. al., 1995) and is strongly linked to the global SST anomalies, land use changes and vegetation-rainfall interaction (Ning et al., 1999; Giannini et al., 2003; Olsson et al., 2005).

Figure 1.2, adapted from NOAA Global Historical Climatology Network[1], shows rainfall in the Sahel (averaged over 20-10^{o}N, 20W-10^{o}E) during June to October from 1900 to 2010. Mean daily temperature approximately varies between a minimum value of 15^{0}C during December/January and a maximum of over 45^{0}C during April/May (Houerou, 1980). The dominant vegetation is composed of grassland, savanna and areas of woodland and shrubland (Anyamba and Tucker, 2005).

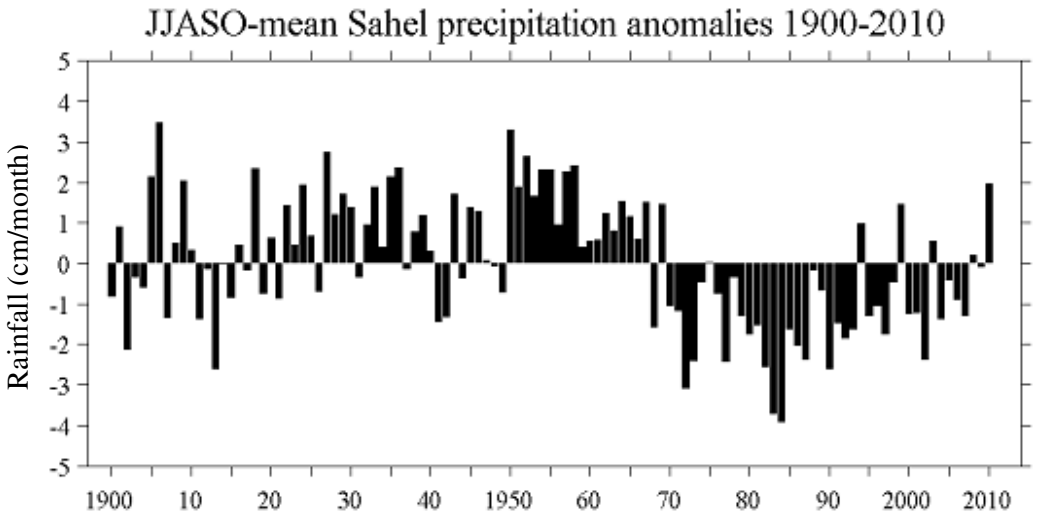

Figure 1.2: Precipitation during Jun-Oct in the Sahel (between 20-10^{o}N and 20W-10^{o}E) during 1900-2010

Due to its dynamic environmental setting, the Sahel has become 'attention-grabbing' to several research communities with regards to vegetation monitoring studies (Seaquist, 2001, Fensholt et al., 2009). It is also known for its persistent drought, which has been observed between 1970's and mid-1990's (Agnew & Chappell, 1999; Heumann et al., 2007). The drought has high recurrence probability, even though rainfall recovery has been observed in 1990's (Agnew & Chappell, 1999). According to Ning et al. (1999), the initial decline in rainfall amount causes changes in the surface and subsequent feedback mechanisms. The low water availability caused by the decreased rainfall reduces vegetation cover, which in turn leads to higher surface albedo and reduced evapo-transpiration. These gradually cause drought and changes in vegetation cover (Ning et al., 1999). Further enhancement of albedo could be caused due to

[1] Available at: http://jisao.washington.edu/data_sets/sahel/

anthropogenic changes in vegetation such as over-cultivation, overgrazing and changes in land use (Giannini et al., 2003, Olsson et al., 2005).

This region is also severely affected by desertification and land degradation (Agnew & Chappell, 1999). In the report by UNEP (1984) it is mentioned that drought, very common in dryland regions, plays a major role in augmenting land degradation. Similarly, reports by UNSO (1997) indicate that the condition in Sudano-Sahel region is caused by severe and extended drought conditions leading to severe damage to land and water resources. In addition to drought, several studies have witnessed a decreasing trend in rainfall (Lamb, 1974; Hare, 1984; Tooze, 1984). Le Barbe´ and Lebel (1997) stated that a decrease in the number of rain occurrences (number of rainy days) is the major cause of the decline in precipitation observed during 1970–1989 in the central Sahel.

The study by Dregne (1986) pointed out human effects in the environment. The effect of drought, which is evident since 1969, only would not cause permanent damage to the ecosystem (Dregne, 1986). The combined effect by mankind (for instance, overgrazing, over-cultivation, deforestation, changes in land use and poor resource management practices) coupled with the long-term drought; cause the region to be more vulnerable (Dregne, 1986; Seaquist, 2001). The effect of civil conflicts and wars in most African countries is also one of the factors leading to worst case of environmental degradation. Such events, though are short-term, their effect to the long-term environmental process is immense (www.drylandscience.org). People will be forced to migrate during such situations leaving the land unattended, and this greatly enhances the resilience of the ecosystem (Olsson, 1993). Moreover, arid and semi-arid regions are resilient due to the spatially diverse rainfall, which compels people to relocate seasonally in search of ambient conditions (Olsson, 1993). Yet, conditions like drought (e.g., Sahel drought in 1968-74) have negative impacts on the livelihood of people (Olsson, 1993).

Overall, loss of vegetation cover in the Sahel cannot be attributed to the long-term effect of the spatially variable rainfall (Nicholson et al., 1998; Tucker and Nicholson, 1999). The vegetation decline is mainly the result of the short-term drought coupled with human effects (Dregne, 1986; Seaquist, 2001; Reynolds, 2004).

However, a closer look at AVHRR satellite data from 1980 to 1997 reveals that a slight greening and moister condition have been observed in the Sahel region (Tucker and Nicholson, 1999). In addition, several other studies have witnessed an increase in NDVI in the Sahel based on the interpretation of NDVI from NOAA AVHRR, Landsat and MODIS sensors. To mention some:

- Eklundh and Olsson, 2003 (using Pathfinder AVHRR NDVI for 1982-1999)
- Sjöström, 2004 (using Landsat, MODIS and AVHRR for 1982 – 2002)
- Hickler et al., 2005 (using NOAA AVHRR for 1982-1998)
- Olsson et al., 2005 (using NOAA AVHRR for the period 1982-1999)
- Herrmann et al., 2005 (using GIMMS AVHRR NDVI for 1982-2003)
- Heumann et al., 2007 (using GIMMS AVHRR NDVI dataset for 1982–2005)
- Fensholt et al., 2009 (using AVHRR GIMMS, MODIS and SPOT data for 2000-2007)
- Huber et al., 2011 (using GIMMS AVHRR NDVI for 1982-2007).
- Fensholt and Rasmussen, 2011 (using GIMMS AVHRR NDVI for 1982-2007)
- Simon and Laura, 2011 (using Meteostat Second Generation, MSG, for 2005-2009)

1.2. Aim and Objectives

The main aim of the study is to assess vegetation change for parts of the Sudan and Chad region, which extends approximately from 10^{o}-20^{o} Northern latitude to 23^{o}-35^{o} Eastern longitude (covered by MODIS tile h20v07) during 2000-2010 (figure 2.1).

The specific objectives are:

- To quantify temporal differences in NDVI and phenological parameters, i.e., annual variation observed within each land cover class over time.
- To quantify the overall spatial difference in phenological parameters (within the image extent).
- To quantify the changes in relation to the amount of rainfall.

Based on the aim and objectives, the study will test the following hypotheses.

$H_0 1$ Temporal changes in NDVI and phenological parameters were not evident within each land cover during 2000-2010.

$H_A 1$ Temporal changes in NDVI and phenological parameters were evident within each land cover during 2000-2010.

$H_0 2$ Spatial variations in phenological parameters were not evident during 2000-2009.

$H_A 2$ Spatial variations in phenological parameters were evident during 2000-2009.

$H_0 3$ The amount of rainfall was not the main driving factor for the observed changes in NDVI and phenological parameters during 2000-2010.

$H_A 3$ The amount of rainfall was the main driving factor for the observed changes in NDVI and phenological parameters during 2000-2010.

1.3. Significance of the study

MODIS is the logical extension of the AVHRR sensor with improved calibration and atmospheric correction (Beck et al., 2006). This study will provide a continuation of vegetation change studies that have mostly been made using NOAA AVHRR data up to 1999. The vegetation during 2000 – 2010 will be observed using 16-day composite NDVI from MODIS. The scope of the study is for part of Sudan and Chad, mainly in the Sahel and Sudanian zone (savanna land cover) (figure 2.1 and figure 2.2).

2. Study area

2.1. Climate

The study area lies in a tropical, hot and strongly seasonal climate. The mean daily temperature approximately ranges from 27ºC to 43ºC (wikipedia.org/wiki/Geography_of_Sudan). The region, which falls within Sudan, extends between desert and semi-dry zones. Mean annual rainfall in the desert ranges from 0 - 100 mm, in the semi-desert 100- 200 mm, in the dry zone 200-400 mm and in the semi-dry 400-600 mm (El Nadi, 2005). The region, which falls within Chad, extends between the Saharan and Sudanian zones. Mean annual rainfall in the Saharan zone is below 200 mm, in the Sahelian zone ranges from 200 - 600 mm and in the Sudanian zone 600 - 1000mm (wikipedia.org/wiki/Geography_of_Chad) (see figure 4.2).

2.2. Topography

The study area has generally flat topography: the elevation ranges from 0 to 3187m and 160m to 3415 m amsl. in the Sudan and Chad, respectively (wikipedia.org).

2.3. Soil

The Sahel region is dominated by sandy soils (luvic arenosol) and black clay soils (vertisols) observed in valleys (Seaquist, 2001). The soils exhibit slightly acidic nature with low nutrient and organic matter content (Houerou, 1980; Seaquist, 2001).

2.4. Vegetation

In the Sahel region, the north-south rainfall gradient is the major factor influencing the vegetation (Justice and Hiernaux, 1986; Seaquist, 2001). The major bioclimatic zones, adapted from Justice and Hiernaux (1986), are indicated in table 2.1.

Table 2.1: Bioclimatic zones and vegetation types in the Sahel

Bioclimatic zone	Delimiting isohyet ($mmyr^{-1}$)	Characteristic vegetation type
Saharan	<150	Sparse perennial grasses and ephemeral annual grasses with shrubs
N. Sahelian	150-300	Annual grasses, sparse shrubs and low trees; a few perennial grasses
Sahelian	300-450	Annual grasses with sparse shrubs and trees; open woodlands in topographic depressions
S. Sahelian	450-600	Annual grasses with open shrubs and trees; open woodlands with a few perennial grasses on the plains
N. Sudanian	600-800	Annual grasses with a few perennials, open shrubs or trees; open woodland on the plains; dense thickets occurring on rock outcrops

The general vegetation of the study area conforms to the information in table 2.1 of bioclimatic zones.

Commonly a time lag of one month is observed between the onset of the rainfall and start of the vegetation season (Eklundh, 1996). The vegetation season June to October is selected to

represent the growing seasons in this study, even though there may be variations across different land cover classes and from year to year.

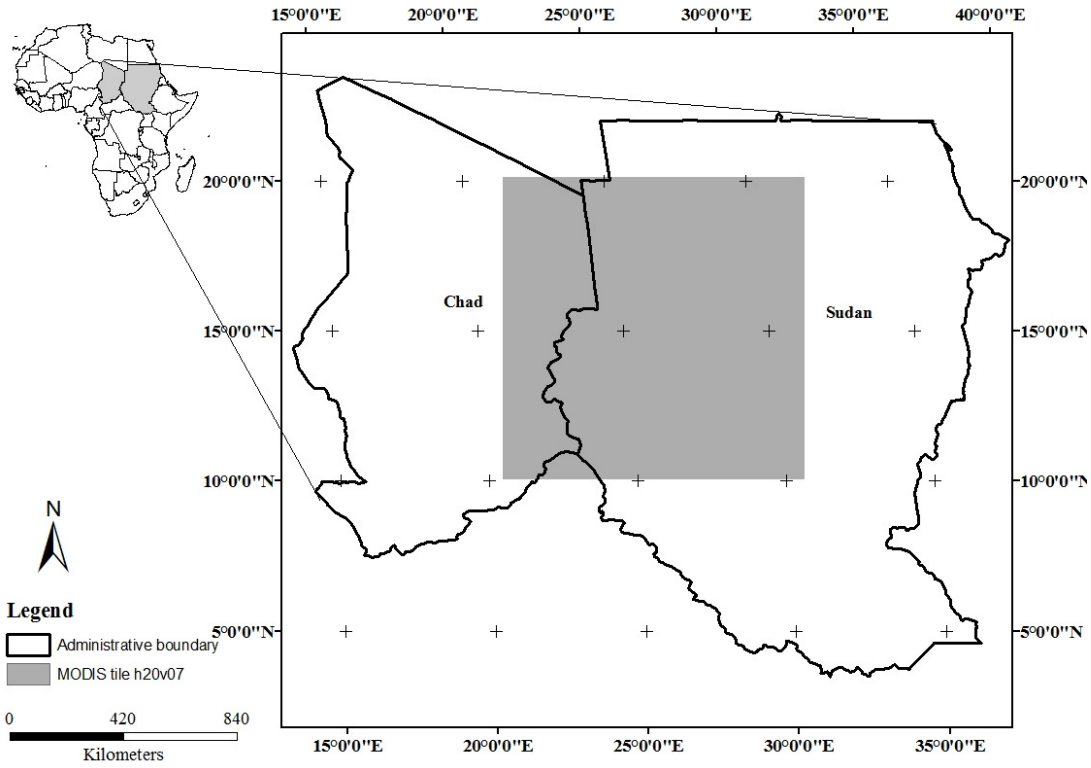

Figure 2.1: Study area

2.5. Land cover

The major land cover classes used in this study are based on IGBP land cover type contained in the MODIS land cover product (MOD12Q1). The study area, corresponding to the MODIS tile h20v07, extends between 10-20^{o}N latitude and 23-35^{o}E longitude (figure 2.2). The description of the land cover classes adapted from Friedl et al. (2002) is given in table 2.2.

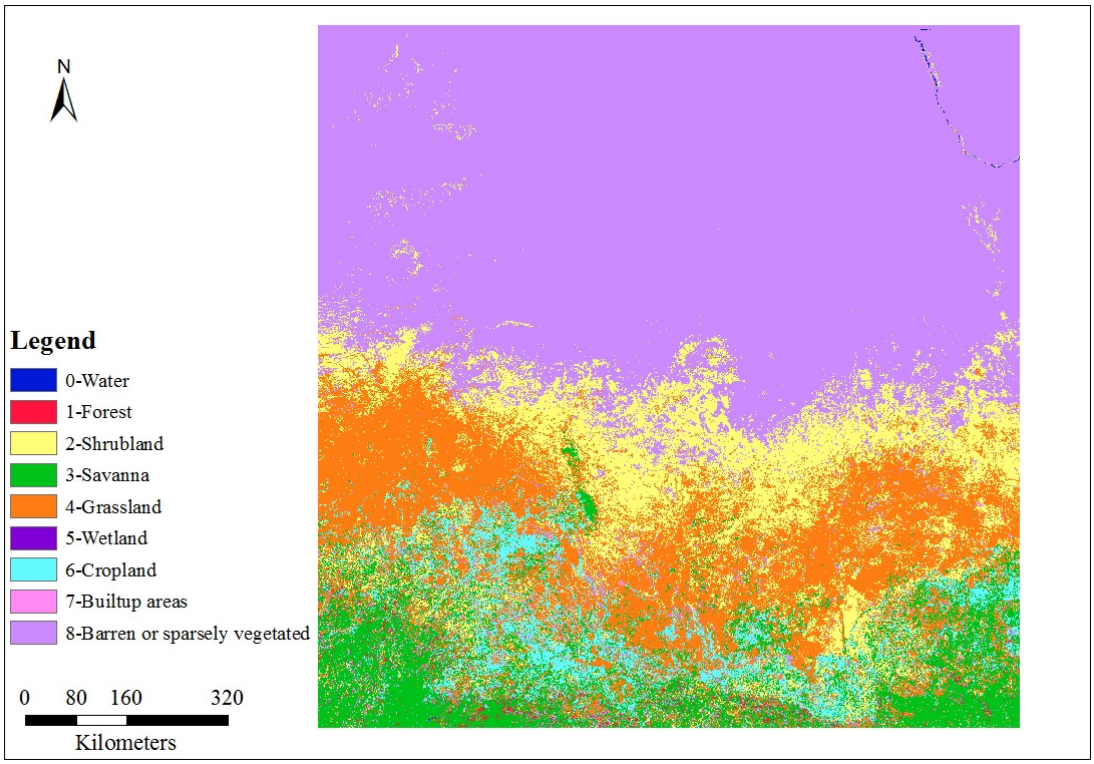

Figure 2.2: MODIS land cover product (MOD12Q1) – IGBP land cover type for 2004 covered by MODIS tile h20v07. Refer figure 2.1 for the administrative boundaries covered by the tile.

Table 2.2: Description of land cover classes according to IGBP land cover type – MODIS land cover product (MOD12Q1) and areal coverage computed for 2004.

Land cover type	Description	Areal coverage (Km^2)
Forest	Areas dominated by needleleaf and/or broadleaf evergreen trees and woody vegetation with >60% cover and >2m height. It also consists of seasonal trees, which have no leaves at some periods during a year.	5513.78
Shrubland	Areas containing shrub canopy cover >10% and height of woody vegetation < 2m.	174382.70
Savanna	Areas containing herbaceous and other understory vegetation with forest canopy cover ranging between 10% - 60% and forest height >2m.	110996.57
Grassland	Areas where herbaceous plants are dominant and are covered by <10% trees and shrubs.	232603.28
Cropland	Areas where crops are cultivated and remain unplanted for certain period before the next cropping season. It also contains a mixture of croplands, forests, shrublands and grasslands (excluding perennial woody crops) each having <60% coverage.	55783.78
Barren or sparsely vegetated	Bare areas with maximum vegetation cover of 10%.	656617.22

3. Theoretical background

3.1. Vegetation indices

Vegetation Indices are empirical measures designed to enhance the measured spectral responses to a reflected vegetation signal. The computation involves combining different wavelength bands, usually red (600-700 nm) and NIR (700-1100 nm) (Huete et al., 1999). According to Jackson et al. (1983, pp 206): "the VI should be particularly sensitive to vegetative covers, insensitive to soil brightness and soil color, little affected by atmospheric, environmental and solar illumination geometry and sensor viewing conditions".

Using these indices, the distinction between vegetation / photosynthetically active biomass and the soil could be made. Hence, changes in land use and vegetation cover density over time could be identified based on the spectral behavior, which is unique for different objects on the surface (Huete et al., 1999).

3.1.1. Normalized difference vegetation index (NDVI)

NDVI is a measure of the presence of vegetation on the surface using spectral properties of the vegetation and ranges between –1.0 and 1.0 (Herrmann et al., 2005; Jönsson et al., 2010). It is used to distinguish vegetation from bare soils; the existence of clouds and water are represented with the negative NDVI, bare soil with low NDVI close to zero and high positive NDVI indicate vegetation (NDVI 0.1-0.5 represent sparse coverage while dense vegetation is represented by NDVI of 0.6 and above, (www.pecad.fas.usda.gov/). Thus, it is possible to determine percentage of vegetation cover on the ground (Herrmann et al., 2005; Salim et al., 2008).
NDVI is computed from the reflectance of the red and NIR spectral bands as:

$$NDVI = \frac{(\mathrm{NIR} - \mathrm{Red})}{(\mathrm{NIR} + \mathrm{Red})}$$

Due to high absorption by leaf pigments, the blue (400-500nm) and red (600-700nm) bands of the visible region show low reflectance. In the NIR region, however, high reflectance is observed with minor absorption caused due to internal cell structure (Tucker et al., 1985). Hence, a contrast between the red and NIR bands is used to give an indication of existing vegetation (Tucker et al., 1985; Huete et al., 1999). It compensates the differences in illumination within the image (resulting from slope and aspect) and between images (due to differences in time and season of image capture). Hence comparison of images captured at different conditions is possible (Katagis et al., 2006).
NDVI is correlated to many biophysical variables in the ecosystem; photosynthetic activity of plants, total vegetative coverage, green biomass, moisture conditions (both soil and plant moisture), plant stress conditions, NPP, LAI and fAPAR but is not a direct measure of such elements (Katagis et al., 2006).

Photosynthetic activity of plants is influenced by several factors such as: climate, nutrients, soil moisture, light, fire, environmental disturbances and the light use efficiency. During photosynthesis, plants utilize absorbed photosynthetically active radiation (APAR), which is the product of incoming PAR and fAPAR, (Seaquist, 2001; Rautiainen et al., 2010).

The gross primary production (GPP), total carbon fixed through photosynthesis, is then given by the Monteith light use efficiency (LUE) model as:

$$GPP\ (gC\ m^{-2}) = \sum \varepsilon . fAPAR\ .PAR$$

Where:

ε = LUE coefficient and depends on maximum biological efficiency of conversion to dry matter and environmental stress scalars (temperature, nutrients and water)

fAPAR = the fraction of PAR absorbed by the canopy and is the product of NDVI and regression coefficients

PAR = incoming radiation (estimated from direct measurements, climate models or remote sensing) (Monteith, 1972; Fensholt et al., 2004).

NPP, net plant growth, is computed by subtracting autotrophic respiration from GPP, which can be estimated using LAI and biomass (Rautiainen et al., 2010).

A near-linear relationship has been identified between NDVI and fAPAR (Huete et al., 1999; Fensholt et al., 2004, 2006). However, the empirical relationships are site-specific as fAPAR is sensitive to soil background, variations in view angle and atmospheric conditions (Fensholt et al., 2004, Rautiainen et al., 2010).

3.1.2. Noise in NDVI

NDVI is affected by existence of cloud and other atmospheric effects, which reduce the contrast between the red and NIR reflectance (Katagis et al. 2006). Atmospheric effects and/or aerosols cause scattering of outgoing path radiances leading to an increase in the red reflectance; while the NIR signals are lowered due to scattering and water vapour absorption (Holben, 1986; Goward et al., 1991; Huete et al., 1999). The amount of surface vegetation is underestimated due to net effect of the atmosphere causing a decrease in NDVI. The increase in red and decrease in NIR reflectance leads to lower NDVI at the top-of-atmosphere than at the top-of-canopy (Guyot et al., 1989; Beck et al., 2006). Therefore, the atmospheric NDVI is generally regarded as subject to negatively biased noise (Guyot et al., 1989; Beck et al., 2006; Hird & McDermid, 2009).

In addition, NDVI is affected by reflectance from the soil surface, effects being greater in less vegetated areas (Huete and Jackson, 1988). Sensor geometry, variations in sun angle, surface anisotropy effects and aerosols are also other sources of variability in NDVI images (Cihlar et al., 1997; Van Leeuwen et al., 1999; Huete et al., 2002; Katagis et al., 2006).

3.2. Moderate Resolution Imaging Spectroradiometer (MODIS)

MODIS is a passive optical sensor recording the amount of electromagnetic radiation reflected and /or emitted from the surface using an array of small sensors and data are stored in the form of digital numbers (modis.gsfc.nasa.gov). It operates on Terra and Aqua satellites; launched first on Terra satellite on 18th of December 1999 and later on Aqua satellite on 4th of May 2002. Both the Terra and the Aqua satellites scan the entire globe every one to two days in sun-synchronous, near polar circular orbits. The Terra satellite passes through the equator in the morning at about 10:30am sweeping in the north-south (descending node) direction, while the Aqua operates in the opposite direction - ascending node - in the afternoon at about

1:30pm (http://modis.gsfc.nasa.gov). This means that MODIS sensor scans the same point on earth both in the morning and afternoon. Hence, the observation of phenomena on land, ocean and in lower atmosphere is possible along with the possibility to predict the occurrence of future events (http://modis.gsfc.nasa.gov).

MODIS has 36 spectral bands covering the visible, nearIR, SWIR/MWIR and LWIR, i.e., 400-14400 nm wavelength ranges of the electromagnetic spectrum. The images are captured at a spatial resolution of 250m for band 1 (red) and band 2 (NIR), 500m (bands 3-7) and 1km (bands 8-36) (http://modis.gsfc.nasa.gov).

3.2.1. Application of MODIS for observing vegetation

The use of remotely sensed data for monitoring vegetation changes is becoming increasingly important (Katagis et al., 2006). The need for global change monitoring and mapping is vital because vegetation influences the geosphere-biosphere-atmosphere interactions, carbon cycle and to global climate change (Strahler et al., 1999; Zhan et al., 2002; Salim et al., 2008). Besides, vegetation monitoring is fundamental to early warning systems, which facilitate the awareness to adverse conditions in food security and disaster (FEWS NET report).

MODIS is designed with seven bands in the reflective region providing specific information about the land surface. The bandwidth maximizes radiometric precision and suppresses atmospheric absorption effects, leading to enhanced vegetation indices (Townshend et al., 1991). Hence, from time series of MODIS NDVI, monitoring changes in vegetation and phenological properties is possible. (Zhang et al., 2003; Gitas et al., 2004; Maselli, 2004).

3.2.2. MODIS NDVI

Large-scale spatial and temporal vegetation comparison is possible using MODIS vegetation index products, based on which interpretation of the terrestrial photosynthetic activity could be made (Huete et al., 1999). However, like any other satellite information-based vegetation monitoring studies, MODIS-based studies are also affected by clouds and other atmospheric disturbances, variations in sun and viewing angles, shadow effects, soil background, variations in moisture conditions, snow, etc. (Cihlar et al., 1997; Van Leeuwen et al., 1999; Huete et al., 2002). Moreover, global bi-directional radiance of the earth's surface using moderate and course resolution satellite sensors, like MODIS, is captured under variable cloud, atmospheric, view and illumination geometry conditions (Huete et al., 1999).

To standardize images captured at different conditions and to minimize the impacts of the above-mentioned disturbances, MODIS images are merged to create a single image in which cloud, atmospheric, sun-sensor angle effects are minimal (Holben, 1986; Van Leeuwen et al., 1999). The process is known as vegetation index compositing, in which a defined temporal interval is represented by a single image (Huete et al., 1999). The composite images are designed in such a way that they are minimally responsive to external influences related to the atmosphere, clouds, viewing and sun angles. Hence, comparing vegetation spatially and temporally is possible (Huete et al., 1999).

3.2.3. Maximum Value Composite (MVC) MODIS NDVI

MODIS – NDVI image composites are based on maximum value compositing (MVC), where the maximum NDVI over 16 days is selected for each pixel. Pixels with minimal cloud and

atmospheric influences are picked (Huete et al., 1999). Standardization of images acquired at different conditions could partly be achieved, as the technique is inclined towards selecting pixels with least optical path lengths (near nadir view and smallest solar angle) (Holben, 1986; Cihlar et al., 1994). The effects of atmospheric contamination and residual clouds are also to a lesser degree; since such effects are more evident at higher optical path lengths (Holben, 1986; Cihlar et al., 1994). This indicates that MVC works best when the major pixel variations arise due to atmospheric effects and path length (near Lambertian surfaces) (Huete et al., 1999).

However, Huete et al. (1999) stated that MVC in MODIS does not consider the anisotropic behaviour of surface conditions arising from canopy structure, shadow and background effects. Due to the wavelength-dependent bidirectional reflectance distribution function (BRDF), the surface anisotropic behaviour is not eliminated during computations of vegetation indices. Surface BRDF signal is attenuated due to atmospheric effects causing off-nadir view and/or sun angles, which result in an increase in path lengths (Huete et al., 1999). Several studies proved off-nadir pixels with large forward-scatter (more shadowed), large view and solar zenith angles are selected by MVC technique (Goward et al., 1991; Moody and Strahler, 1994; Cihlar et al., 1994, 1997; Huete et al., 1999). These pixels are not necessarily devoid of clouds and atmospheric effects (Huete et al., 1999). Overall, the maximum value NDVI selected is subject to both atmospheric and anisotropic (bi-directional) properties and might render unpredictable results (Huete et al., 1999).

3.3. TIMESAT

Phenological vegetation characteristics cannot be directly extracted from coarse resolution satellite data (Heumann et al., 2007). Nevertheless through pixel-wise analysis of time series of NDVI, an indication of changes in phenological parameters and dynamics of vegetation in an area could be captured (Badeck et al., 2004). The extraction of the required information becomes complicated due to atmospheric influences and sun-sensor viewing geometries, which cause noisy patterns (Huete et al., 1999). To extract required information by reducing the impacts of noise, TIMESAT could be used. TIMESAT is a program package developed for extracting seasonality parameters from a series of data captured using remote sensing techniques over time and provides smooth time series by fitting different model functions to the time series (Jönsson & Eklundh, 2002, 2004; Eklundh and Jönsson, 2009).

Vegetation index images are arranged in two-dimensional spatial arrays and each image represents a specific time period (figure 3.1). TIMESAT extracts vegetation index at a specific pixel (j,k) in a series of time, which gives a sequence of raster data values for that pixel (Eklundh and Jönsson, 2009). Then, mathematical models are applied to smoothen the noisy patterns in the dataset. Subsequently, seasonality parameters are extracted: season start, end, length, base level, amplitude, derivatives, integrals and asymmetry for the data in the time series covering full seasons. That is, parameters will be extracted for n-1 years (where, n is the number of years in the input time series) (Eklundh and Jönsson, 2009).

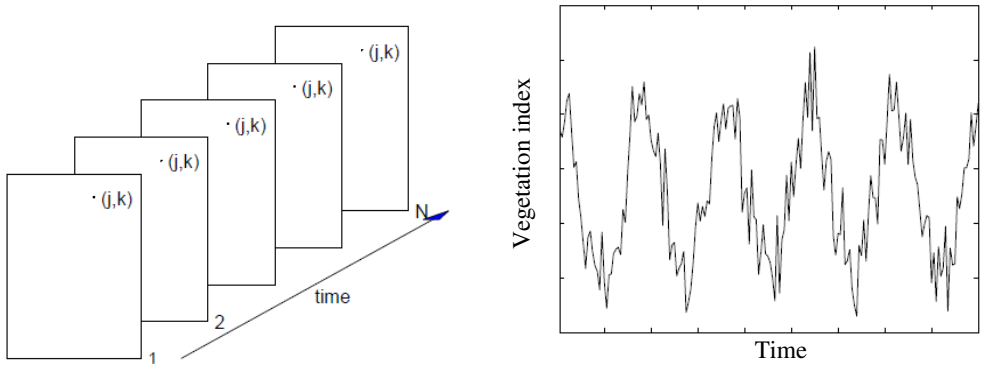

Figure 3.1: NDVI images for pixel (j.k) over time (left) and the corresponding extracted time series (right)

Source: Eklundh and Jönsson, 2009

The description of the parameters as defined by Eklundh and Jönsson (2009) and, Jönsson, and Eklundh (2004) is given as follows (see also figure 3.2 adapted from Eklundh and Jönsson (2009).

- **Start of a season**: indicates the point in time at which an increase by a certain defined value is observed. It gives the proportion of seasonal amplitude measured from the left minimum value. In other words, it is the time when the photosynthetic activity / growth of vegetation starts.
- **End of a season**: indicates the point in time at which a decrease by a certain defined value is observed. It gives the proportion of seasonal amplitude measured from the right minimum value. In other words, it is the time when the photosynthetic activity / growth of vegetation ends.
- **Length of a season**: indicates the time from the start to the end of growing season and determines the amount of moisture available for vegetation.
- **Base level**: indicates the average of minimum values of the start and end of the growing season.
- **Amplitude of a season**: indicates the difference between the maximum value and base level.
- **Integrals**: An estimate of the net primary production can be made using integrated NDVI as these give the cumulative NDVI over the growing season (Jönsson and Eklundh, 2004). The active vegetation cover in a season is encompassed by the area between the fitted/ smooth function and the base level and is termed as **small integral**. Similarly, the area between the fitted function and the zero level (figure 3.2) gives the total vegetation in an area (including all year round green biomass) and is termed as the **large integral**.
- **Rate of increase at season start:** indicates the ratio of the difference of the left 80% and 20% levels to the corresponding time variation and is given by the **left derivative.**
- **Rate of decrease at season end:** indicates the ratio of the difference of the right 80% and 20% levels to the corresponding time variation and is given by the **right derivative**.
- **Asymmetry:** indicates the slope difference between the start and end of a growing season.

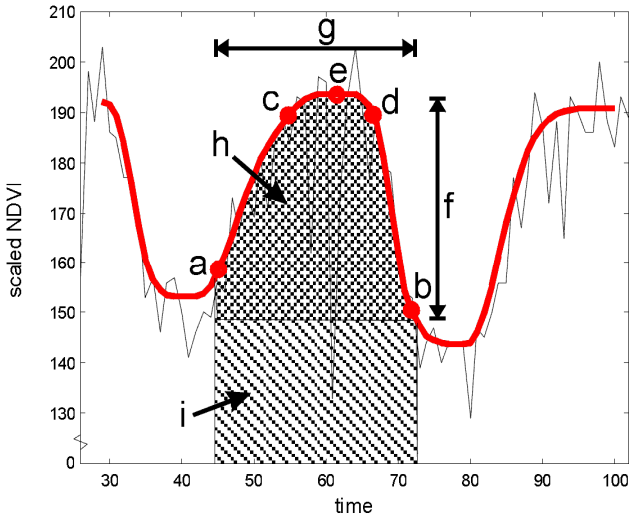

Figure 3.2: Seasonality parameters from TIMESAT: a) Start of season b) End of season c) Left 80% level d) Right 80 % level e) Peak f) Amplitude g) Length of season h) Small integral i) Large integral

3.3.1. Fitting functions

TIMESAT employs functions, capable of capturing seasonal and inter-annual variations, as compared to other approaches that are based on Fourier methods (Eklundh and Jönsson, 2009).

Adaptive Savitzky Golay filter

The TIMESAT Savitzky Golay filter is based on a weighted moving average, in which local fits are employed for a certain window. It preserves the area and peak of a season (Chen et al., 2004). The size of the window selected plays a major role in the capacity of the model to maintain signal integrity of the dataset (Eklundh and Jönsson, 2009). A large window renders a smooth curve but affects the temporal structure of the data while a small window preserves the noise in the original dataset (Chen et al., 2004; Jönsson & Eklundh, 2004; Hird & McDermid, 2009; Jönsson et al., 2010).

The Savitzky Golay filter is not recommended for noisy time series data (Jönsson and Eklundh, 2002). Noise could arise due to phenological differences or biogeographic regions behaving differently to different noise reduction methods (Hird & McDermid, 2009). When selecting such a method, the strength and quality of the noise, which affects the performance of the employed method, must be looked at carefully.
In addition, the Savitzky Golay filter gives an over-estimated fit for the season of high NDVI (NDVI during the growing season) and is affected by abrupt dips in the NDVI (Hird & McDermid, 2009). Nevertheless, the method considers negatively biased noise, maintains higher values and is able to minimize overall noise fairly well (Chen et al., 2004; Hird & McDermid, 2009). Even so, Hird & McDermid (2009) stated that their study is based on a discrete single growing season and their observation might not be appropriate to regions of multiple or no distinct seasonality. .

Asymmetric Gaussian function

The asymmetric Gaussian function is based on a non-linear least square global model function and is capable of capturing seasonal variations (Jönsson and Eklundh, 2002). However, it is unable to distinguish whether the observed maxima and minima are from seasonal variations or from noise in the dataset (Jönsson and Eklundh, 2002).

Double logistic function

Similar to the asymmetric Gaussian function, the double logistic function is also based on least square fitting. The data sets smoothed using this method show reasonable growing season length and other phenological parameters and the general signal integrity is preserved (Jönsson et al., 2010). In addition, distinction between autumn and spring timing could be observed as it handles outliers effectively (Beck et al., 2006).
In the study by Beck et al. (2006), it is observed that a major source of error in double logistic function is that it employs equal fitting values at the start and end of the season. This overestimates values before start of the season and underestimates at season start (Beck et al., 2006).

Similarly, several studies agree that overall noise reduction and integrity of the data is achieved best when asymmetric Gaussian and double logistic functions are implemented (Hird & McDermid, 2009; Jönsson and Eklundh, 2002, 2004; Beck et al., 2006). This could be due to the fact that upper envelope of NDVI is preserved leading to reasonably good fits during the growing season (season of high NDVI). In addition, inactive vegetative seasons (NDVI during winter) are distinctively estimated and hence, negatively biased noise is minimized and the fit of either of these methods is not influenced by abrupt dips in the NDVI (Hird & McDermid, 2009).

3.3.2. Assumptions of TIMESAT

TIMESAT assumes that the signals, on which the fitting functions are applied, represent vegetation. (Jönsson and Eklundh, 2002). Besides, the data in the time series are considered as evenly sampled or TIMESAT ignores the effects of unevenly sampled MVC NDVI datasets (Eklundh and Jönsson, 2009).

4. Materials and methods

4.1. Remote sensing data

4.1.1. MODIS – NDVI

16-day maximum value composite NDVI images (23 scenes represent one calendar year) were acquired from NASA's WIST and ECHO data centres[2]. The images are radiometrically and atmospherically corrected and gridded into Sinusoidal projection. The main properties of the images are shown in table 4.1.

Table 4.1: Properties of MODIS-NDVI product (MOD13Q1) from Terra satellite

Parameters	Property
Data format	Hierarchical Data Format (HDF)
Spatial resolution	250 m
Tile	h20v07
Projection	MODIS Sinusoidal
Scaling factor	10000
Offset	0
Quality flag[3]	- Reliable VI, most pixels are free of clouds and have low aerosol. - Vegetation indices match with land surface biophysical variables and show good agreement with that adjusted for nadir.

For preliminary analysis, 8-day composite NDVI computed from MODIS surface reflectance product (MOD09A1) was also used to see the effect of the length of compositing periods (see appendix E). This dataset has 500 m spatial resolution (see Sjöstöm et al., 2009 for details) and one calendar year is represented by 46 images.

4.1.2. MODIS – Land cover product (MOD12Q1)

The MODIS land cover product based on data from Terra satellite (MOD12Q1) – IGBP land cover type of 1-km spatial resolution (tile h20v07) was acquired from WIST and ECHO data centers[2].

4.2. Precipitation data

Time series of daily rainfall estimates for 2001-2010 covering the whole part of the study area was acquired from Famine Early Warning System Network (FEWS NET)[4] (CPC/Famine Early Warning System Daily Estimates). The rainfall grids have a spatial resolution of 0.1^{o}x 0.1^{o} and the rainfall estimate is based:

- WMO Global Telecommunication Stations (GTS) daily rain gauge data
- Advanced Microwave Sounding Unit (AMSU) microwave satellite precipitation estimates
- Special Sensor Microwave/Imager (SSM/I) satellite rainfall estimates
- GOES Precipitation Index (GPI) cloud-top IR temperature precipitation estimates.

[2] https://wist.echo.nasa.gov/api/
[3] Detailed information is available at http://modis-250m.nascom.nasa.gov/cgi-bin/QA_WWW/detailInfo.cgi?prod_id=MOD13Q1&ver=C5
[4] http://earlywarning.usgs.gov/fews/africa/index.php

The daily precipitation data were computed first by combining the rainfall estimates from the three satellites (GPI, SSM/I and AMSU) and later were merged with station data (GTS) to establish the final rainfall in millimeters (mm) (Xie and Arkin, 1996).

4.3. Methods

Time series analysis of NDVI during 2000-2010 was made for the major land cover classes. The methods employed in the study include: stratification and selection of pixels and TIMESAT procedures, which involve pre-processing, processing and post-processing. The overall procedure is briefly illustrated by the flow chart in figure 4.1.

4.3.1. Stratification of the study area

The stratification of the regions for selecting sample pixels was made based on MODIS land cover product (MOD12Q1) – IGBP land cover type for 2004 (section 2.5). This global product originally contains 16 land cover classes and was reclassified into 8 classes (appendix table A1). In this study, shrubland, savanna, grassland, cropland and barren or sparsely vegetated land cover classes are considered. Forest land cover class is not analyzed since homogenous area of 5 by 5 pixels could not be found.

4.3.2. Selection of sample pixels

In order to be able to digitize homogenous area of 5 by 5 pixels from each land cover class (figure 2.2), the geometric resolution of the land cover product was re-computed to correspond to that of the NDVI product. The selected sample pixels have a spatial resolution of 5x250m (1.25km).

Figure 4.2 shows the location of sample pixels with respect to North-South rainfall variation and the coordinates of the sample sites are indicated in table 4.2.

Table 4.2: Location of 5x5 sample pixels from different land cover classes and the corresponding mean annual rainfall in mm. during 2001-2010.

Land cover type	Latitude	Longitude	Mean annual RF in mm (2001-2010)
Shrubland	26.699	14.261	147.0
Grassland (Sudan)	30.478	13.288	285.9
Cropland	23.474	12.699	642.3
Grassland (Chad)	21.219	13.715	469.7
Savanna	21.636	10.442	733.5
Barren/sparsely vegetated	28.317	17.277	25.0

The NDVI images are in MODIS Sinusoidal reference system. For consistency, the vector files containing sample pixels, the IGBP land cover product and the rainfall grids were converted to have the same reference system and was used throughout the study.

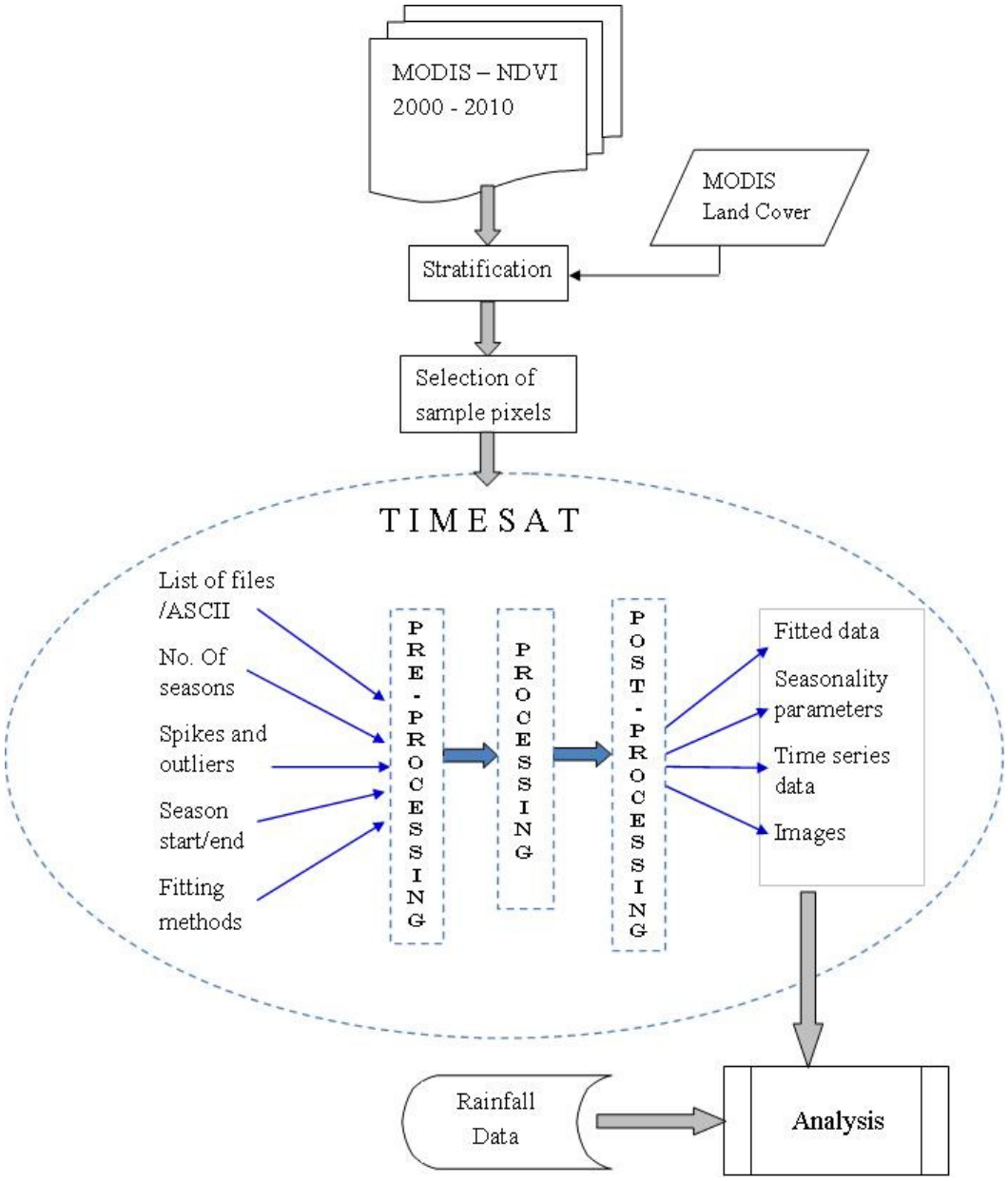

Figure 4.1: Method flow diagram

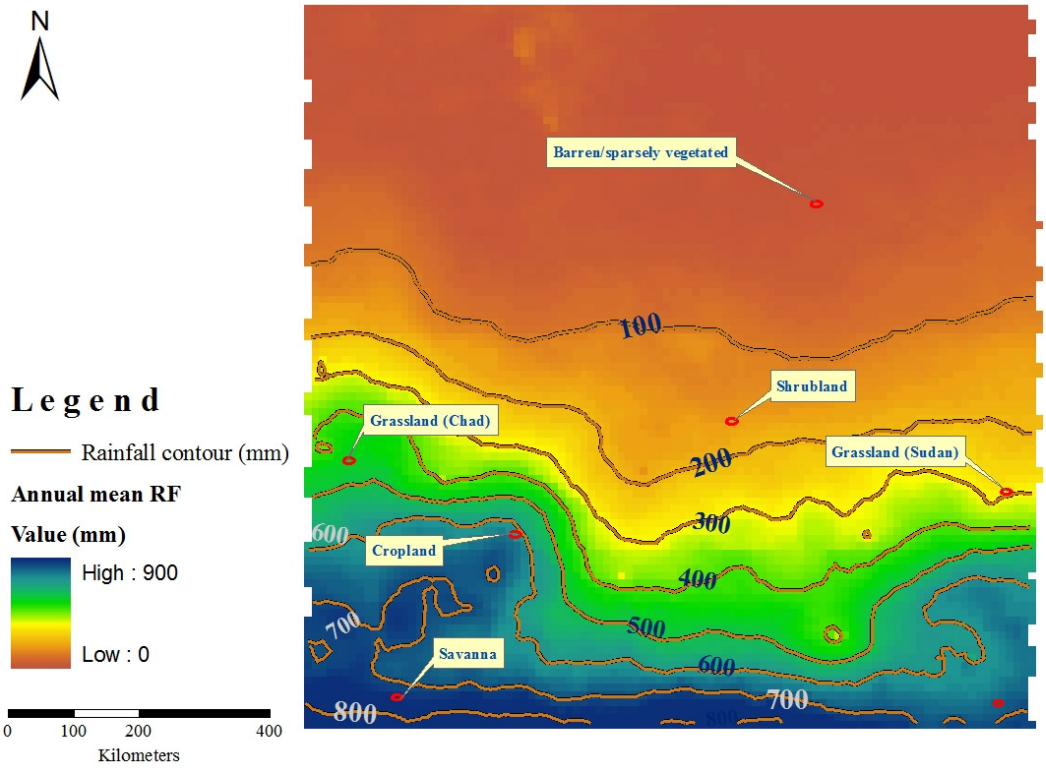

Figure 4.2: Annual mean rainfall (2001-2010) and location of sample pixels

4.3.3. Time series analysis using TIMESAT

To observe the changes over time, series of NDVI for the time period 2000-2010 were analysed using TIMESAT. The processing schemes in TIMESAT are categorized into: data preparation, processing and post-processing stages.

Data preparation / Pre-processing

At the preparation stage, a file list of images over the time period was created. TIMESAT requires full data set for each year (Eklundh and Jönsson, 2009). However, the first three composite images in the time series, Julian days 1 - 48 (Jan 1st– Feb 17th, 2000) were not available. The first image in the time series (Julian day 49–64 / Feb 18th - Mar 4th) was, therefore, duplicated to compensate these missing images, assuming similar vegetation cover exist between Julian days 1 – 64.
To define the parameters for analysis, different TIMESAT parameters were tested to come up with representative fits.
Similarly, 8-day composite NDVI were extracted for each land cover over 2000-2010 (for preliminary analysis) and were converted to ASCII for further processing in TIMESAT.

Setting parameters and fitting methods

i. Determination of number of seasons

The number of seasons in TIMESAT preparation stage was generally determined by observing the first and second maxima in the fit. If the amplitude of the first peak is higher

than that of the second, it is considered as a single season and the seasonal parameter is set to 1. Similarly, if the first maximum has lower amplitude than the second, it is considered as dual vegetation seasons and the parameter value is set to 0 (Jönsson and Eklundh 2004). In all cases, a single season was observed.

ii. Spikes and outliers

In the dataset, unexpected change (extreme deviation from the mean) could be observed due to clouds, agricultural activities and/or the image compositing technique (see section 3.2.3 for details). To remove these spikes and outliers (since no quality data has been used to suppress such effects by assigning less weight), median filtering with a parameter value of 2 was implemented. That is, values two standard deviations away from the median are considered as outliers and were not taken into account (Eklundh and Jönsson, 2009).
To account the effect of the negatively biased noise, adaptation to the upper envelope was set to suppress the effect of low data values. This parameter was given a value of 2 or 3 depending on the condition of the data set.

iii. Thresholds for Season start and end

The time between the start and end of the growing season determines the amount of moisture available for vegetation, which in turn influences the length of the growing season. . Determination of the thresholds for start and end of the growing seasons (left and right minimum values) were made to conform to the seasonal behaviour of the land cover classes and to the assumed vegetation season (June-October) stated in section 2.4.

iv. Fitting methods

The seasonality parameters for each land cover were based on different noise reduction techniques, which provide smooth annual time series on pixel-by-pixel basis. Seasonality parameters could not be extracted for barren or sparsely vegetated land cover class, since no growing season could be identified. The parameters used in the analysis for each land cover class (implemented for both 16 and 8day composite images) are indicated in table 4.3 and all were based on defined minimum to improve the fit.

Table 4.3: Parameters used for processing in TIMESAT

Land cover classes	Parameters						
	Spike method	Seasonality parameter/ min value	Envelop iterations	Adapta-tion Strength	Fitting function	Season start	Season end
Shrubland	Median filter (2)	1/ 0.125	2	3	Assymetric Gaussian	0.3	0.45
Savanna	Median filter (2)	1 / 0.2	2	2	Double logistic	0.25	0.45
Grassland (Chad)	Median filter (2)	1 / 0.2	2	2	Savitzky Golay (window 3)	0.2	0.4
Cropland	Median filter (2)	1/ 0.2	2	4	Assymetric Gaussian	0.3	0.4
Grassland (Sudan)	Median filter (2)	1 / 0.2	2	2	Savitzky Golay (window 3)	0.2	0.4

Sensitivity analysis to the adaptation strength parameter

To see the effect of the adaptation strength (which enables to suppress the effect of low data values), a preliminary analysis was made for the savanna and shrubland land cover classes.

NDVI in shrubland did not show a noticeable response to adaptation strength values (appendix B1 shows the response of the large integral to adaptation strength values of 3 and 4).
In savanna, the small integral and season length did not respond much to adaptation strength values (see appendix B2). On the other hand, the seasonal amplitude and the large integral were sensitive to adaptation strength values (appendix B3 and B4). These variations could indicate that the effect of TIMESAT parameter settings was negligible compared to the intrinsic spatial and temporal variation in each land cover class.

Data processing

The processing procedure involves computation of seasonality parameters using the parameters in table 4.3 for each pixel in the selected land cover classes.

Post-processing

The extraction and display of seasonality parameters based on fitted functions was done during the post-processing procedure.

4.3.4. Analysis

Temporal variation

The observation of changes over time was made using smoothed NDVI and seasonality / phenological parameters. The average of the time series over the 5x5 pixel areas were computed and statistical test performed to examine if the changes were significant. The mean of 2000-2005 was compared against that of 2006-2010 for the smoothed NDVI. However for seasonality parameters, the mean of 2000-2004 was compared against 2005-2009, since TIMESAT computes seasonality parameters one year less than the input years (n-1 years). The statistical test was based on t-test (95% confidence level and n-2 degrees of freedom) and was performed under the assumption that the datasets are normally distributed, independent and have equal sample sizes.

The outputs in start, end and length of growing seasons were interpreted by multiplying by the index value (number of composite images) to obtain the respective Julian days. For instance, season start value of 10.41 in the 16-day composite images indicates start of the growing season at Julian day 167 or Jun 16 (10.41 multiplied by 16).

Spatial variation

The observation of the variation over space was done using land cover data. During pre-processing, the land cover map's data type (image format) was converted to be compatible to the data type of NDVI images. The setting file for processing the entire image was then created by stating the number of classes in the land cover map and employing land cover class specific settings as indicated in table 4.3.

The observation of changes in spatial variation (within the image extent) overtime was then made based on the seasonality parameters: seasonal amplitude, length of the growing season and small integral. The mean value of each of the parameters was computed by dividing the time series into two halves. That is, the mean of 2000-2004 was compared against mean of 2005-2009 by computing the difference of the means.

Occurrence of rainfall

Vegetation in an area depends on natural (such as rainfall and temperature), anthropogenic and other factors such as fire, which impose changes through replacement of the natural vegetation by cultivated fields (Eklundh, 1996). To explain the observed changes, since vegetation in this region is highly dependent on rainfall, the amount of rainfall was analyzed.

Annual total rainfall and the amount during the rainy season May-October were extracted for each of the 5x5 pixels representing each land cover during 2001-2010 (no data could be found for 2000). The rainfall was also tested statistically to see whether there have been significant changes in the amount of rainfall. Similar to the NDVI, the statistical analysis is based on 95% confidence level t-test with n-2 degrees of freedom.

5. Results

5.1. NDVI temporal variation in different land cover classes

5.1.1. Smoothed NDVI

NDVI for the whole season

The temporal variations in fitted NDVI for the whole season and for each land cover during 2000-2010 are presented in figures 5.1 and 5.2.

The overall variability, the median and the rate of change in each land cover class over time could be seen from the boxplots in figure 5.1. Symmetrically all the land cover classes show positive skewness (skewed to the right) implying abrupt increase and gradual decline in NDVI over time.

The fitted NDVI during 2000 – 2010 is summarized below and all, with the exception of the trend in shrubland, were not statistically significant (see appendix D).

- In shrubland, the NDVI ranged between 0.15 – 0.35 and a significant increase by 0.03 units was observed (figure 5.2A).
- In grassland (Sudan), the value was between 0.15 – 0.45 and a slight decline by about 0.008 units was observed (figure 5.2B).
- In grassland (Chad), the value was between 0.2 – 0.5 and an increase by about 0.03 units was observed (figure 5.2C).
- In the cropland, the value was between 0.2 – 0.8 and a steady condition was observed (figure 5.2D).
- In Savanna, the value was between 0.2 – 0.9 and an increase by about 0.07 units was observed (figure 5.2E).

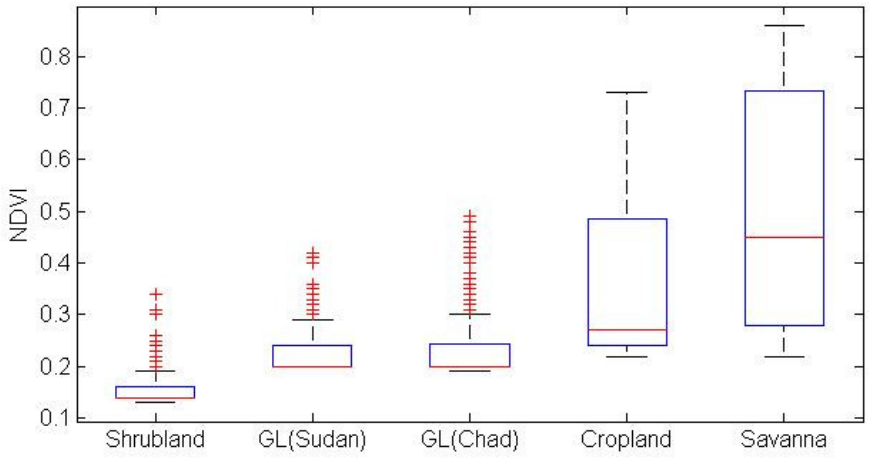

Figure 5.1: Boxplots indicating the fitted NDVI for the whole season in different land cover classes during 2000-2010. Boxes indicate the variability (difference between upper and lower quartiles), median (middle 50% of the data), outliers, the range and symmetry indicated by the extension of the whiskers.

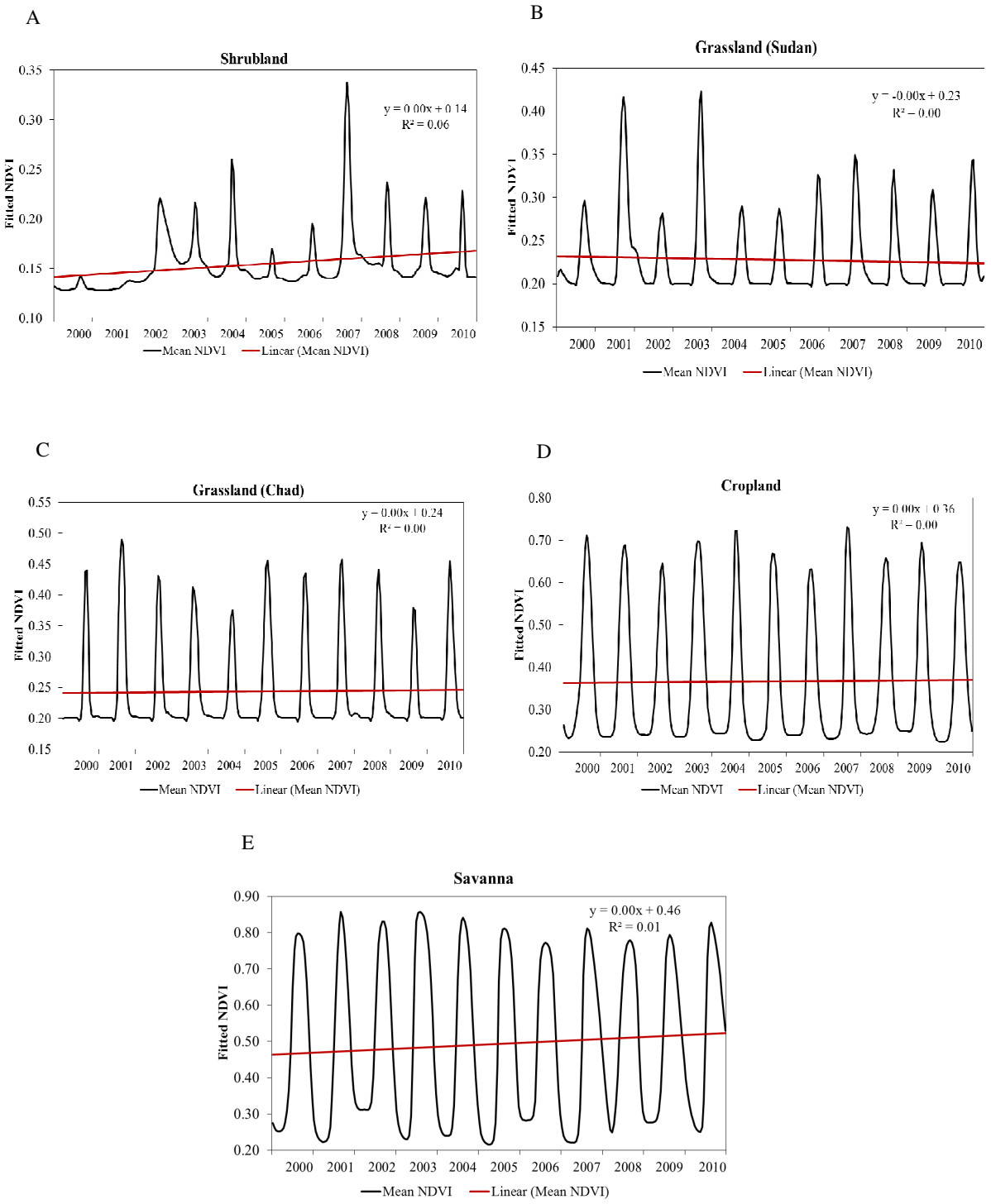

Figure 5.2: Temporal NDVI variation in shrubland (A), grassland_Sudan (B), grassland_Chad (C), cropland (D) and savanna (E) during 2000-2010 fitted using different fitting methods as indicated in table 4.3.

NDVI during the growing season

The fitted NDVI during the growing season June-October (image 12-19) for each land cover class is indicated in figure 5.3.

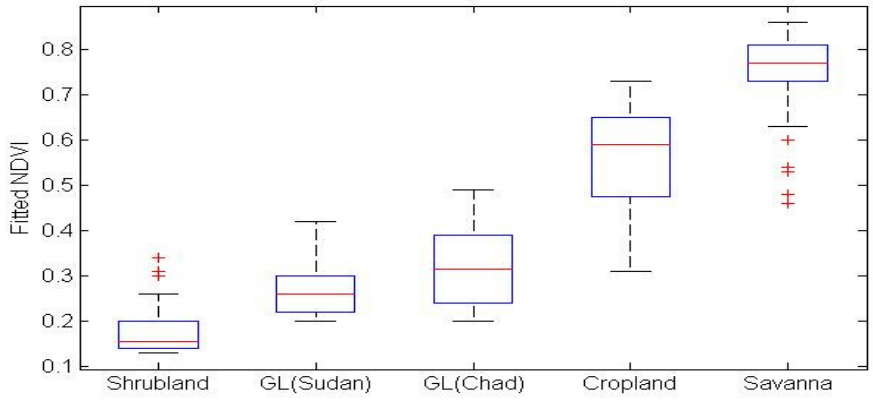

Figure 5.3: Boxplots showing the fitted NDVI during the growing season (June-October) in different land cover classes during 2000-2010 (refer figure 5.1 caption for description).

5.1.2. Seasonality parameters

Using the parameter settings employed in TIMESAT (table 4.3), the seasonality parameter outputs for each land cover class on yearly basis are presented in tables 5.1-5.5.

Table 5.1: Seasonality parameters for shrubland based on Asymmetric Gaussian function

Season	Start (Julian days)	Start (Date)	End (Julian days)	End (Date)	Length (Days)	Base val.	Peak val.	Ampl	Large Integral	Small Integral
2000	230	Aug17	317	Nov12	87	0.13	0.14	0.01	0.97	0.07
2001	198	Jul17	379*	Jan13	181	0.13	0.14	0.01	1.81	0.06
2002	251	Sep8	308	Nov4	57	0.15	0.30	0.15	1.16	0.43
2003	234	Aug22	289	Oct16	55	0.15	0.22	0.07	0.95	0.22
2004	238	Aug25	282	Oct8	45	0.14	0.27	0.13	0.87	0.31
2005	212	Jul31	301	Oct28	89	0.14	0.16	0.02	1.06	0.08
2006	261	Sep18	336	Dec2	75	0.14	0.22	0.08	1.17	0.31
2007	223	Aug11	306	Nov2	84	0.15	0.34	0.19	1.90	0.85
2008	250	Sep6	318	Nov13	69	0.15	0.23	0.08	1.18	0.31
2009	240	Aug28	350	Dec16	110	0.14	0.23	0.10	1.81	0.57

** End of the growing season occurs in the following year and is illogical since no vegetation season was captured.*

Table 5.2: Seasonality parameters for grassland (Sudan) based on adaptive Savitzky-Golay filtering

Season	Start (Julian days)	Start (Date)	End (Julian days)	End (Date)	Length (Days)	Base val.	Peak val.	Ampl	Large Integral	Small Integral
2000	215	Aug2	327	Nov22	113	0.20	0.30	0.10	2.30	0.51
2001	220	Aug8	331	Nov27	110	0.20	0.41	0.21	2.94	1.15
2002	215	Aug3	319	Nov14	104	0.20	0.29	0.09	2.04	0.45
2003	235	Aug23	314	Nov9	79	0.20	0.40	0.20	2.12	0.73
2004	249	Sep6	334	Nov30	84	0.20	0.28	0.08	1.91	0.32
2005	229	Aug17	330	Nov26	101	0.20	0.28	0.08	1.96	0.38
2006	248	Sep5	340	Dec6	91	0.20	0.32	0.12	2.13	0.56
2007	231	Aug19	331	Nov27	101	0.20	0.34	0.14	2.29	0.70
2008	240	Aug28	322	Nov17	81	0.20	0.35	0.15	1.96	0.58
2009	229	Aug17	328	Nov24	99	0.20	0.34	0.14	2.22	0.65

Table 5.3: Seasonality parameters for grassland (Chad) based on adaptive Savitzky-Golay filtering

Season	Start (Julian days)	Start (Date)	End (Julian days)	End (Date)	Length (Days)	Base val.	Peak val.	Ampl	Large Integral	Small Integral
2000	210	Jul28	281	Oct7	71	0.20	0.47	0.27	2.20	1.03
2001	197	Jul16	287	Oct14	90	0.20	0.53	0.33	2.87	1.49
2002	213	Aug1	288	Oct15	76	0.20	0.48	0.28	2.43	1.04
2003	192	Jul11	293	Oct20	101	0.20	0.45	0.25	2.84	1.25
2004	214	Aug1	297	Oct23	84	0.20	0.45	0.25	2.37	0.99
2005	193	Jul12	301	Oct28	108	0.19	0.48	0.29	3.06	1.52
2006	221	Aug9	303	Oct30	82	0.20	0.48	0.29	2.51	1.14
2007	205	Jul24	322	Nov18	116	0.20	0.38	0.18	2.77	0.99
2008	234	Aug21	312	Nov7	78	0.20	0.43	0.24	2.11	0.92
2009	235	Aug23	307	Nov3	72	0.20	0.43	0.24	2.25	0.88

Table 5.4: Seasonality parameters for cropland based on Asymmetric Gaussian function

Season	Start (Julian days)	Start (Date)	End (Julian days)	End (Date)	Length (Days)	Base val.	Peak val.	Ampl	Large Integral	Small Integral
2000	183	Jul1	312	Nov7	129	0.23	0.70	0.47	5.33	3.05
2001	179	Jun28	311	Nov7	132	0.23	0.66	0.43	5.64	3.11
2002	199	Jul18	308	Nov4	109	0.23	0.65	0.42	4.10	2.26
2003	185	Jul4	315	Nov11	130	0.22	0.68	0.46	5.42	3.19
2004	210	Jul28	311	Nov6	101	0.22	0.68	0.45	4.06	2.28
2005	210	Jul29	329	Nov25	118	0.23	0.65	0.42	4.59	2.57
2006	218	Aug6	335	Dec1	115	0.22	0.59	0.36	4.30	2.29
2007	223	Aug11	325	Nov21	103	0.23	0.69	0.46	4.23	2.41
2008	218	Jul5	346	Dec11	128	0.23	0.65	0.42	5.12	2.78
2009	217	Aug5	329	Nov25	112	0.22	0.71	0.49	4.80	2.79

Table 5.5: Seasonality parameters for savanna based on Double Logistic function

Season	Start (Julian days)	Start (Date)	End (Julian days)	End (Date)	Length (Days)	Base val.	Peak val.	Ampl	Large Integral	Small Integral
2000	167	Jun15	348	Dec13	181	0.23	0.80	0.58	8.56	5.60
2001	187	Jul6	335	Dec1	148	0.24	0.84	0.60	7.27	4.62
2002	192	Jul11	350	Dec16	158	0.27	0.85	0.58	7.94	4.69
2003	163	Jun12	348	Dec14	185	0.27	0.87	0.60	9.86	6.10
2004	178	Jun26	345	Dec10	168	0.24	0.84	0.59	8.14	5.22
2005	186	Jul5	351	Dec17	164	0.24	0.82	0.58	8.12	5.19
2006	170	Jul19	349	Dec15	179	0.24	0.84	0.60	8.76	5.62
2007	208	Jul27	376*	Jan11	167	0.23	0.83	0.60	8.30	5.28
2008	168	Jun16	358	Dec23	191	0.27	0.78	0.52	8.50	5.00
2009	195	Jun14	377*	Jan12	182	0.27	0.79	0.52	8.47	4.94

** End of the growing season occurs in the following year*

The seasonality parameter outputs: start, end and length of the growing seasons, amplitude and integrals for all land cover classes are presented in figures 5.4-5.9 (see appendix C for the plots in each land cover class on yearly basis).

Start of the growing season

The start of the growing season for each land cover is indicated in figure 5.4. Over the time period 2000-2009, 40 days delay in the start of the growing season in shrubland, 20 days delay in grassland (Sudan), 28 days delay in grassland (Chad), 44 days delay in cropland and 13 days delay in savanna were observed. The statistical test outputs show that only cropland was statistically significant (see appendix D).

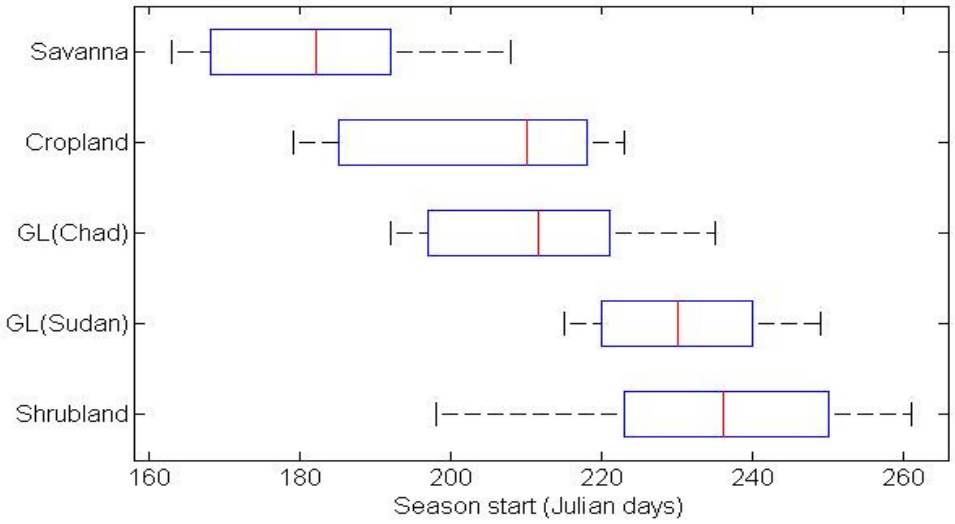

Figure 5.4: Boxplots showing the start of the growing season in different land cover classes during 2000-2009 (refer figure 5.1 caption for description).

End of the growing season

The end of the growing season for each land cover is indicated in figure 5.5. Over the time period 2000-2009, a steady condition in the end of the growing season in shrubland, 4 days delay in grassland (Sudan), 34 days delay in grassland (Chad), 30 days delay in cropland and 31 days delay in savanna were observed. The end of the growing season for grassland (Chad), cropland and savanna were proved to be statistically significant (see appendix D).

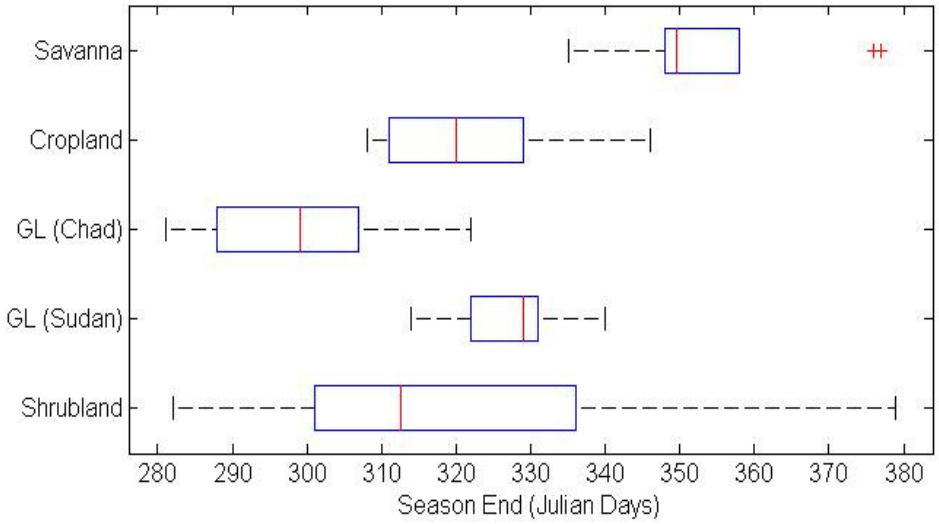

Figure 5.5: Boxplots showing the end of the growing season in different land cover classes during 2000-2009 (refer figure 5.1 caption for description).

Length of the growing season

The length of the growing season for each land cover is indicated in figure 5.6. Over the time period 2000-2009, 13 days decrease in the length of the growing season in shrubland, 15 days decrease in grassland (Sudan), 5 days increase in grassland (Chad), 13 days decrease in cropland and 19 days increase in savanna were observed. The statistical test outputs show that none was statistically significant (see appendix D).

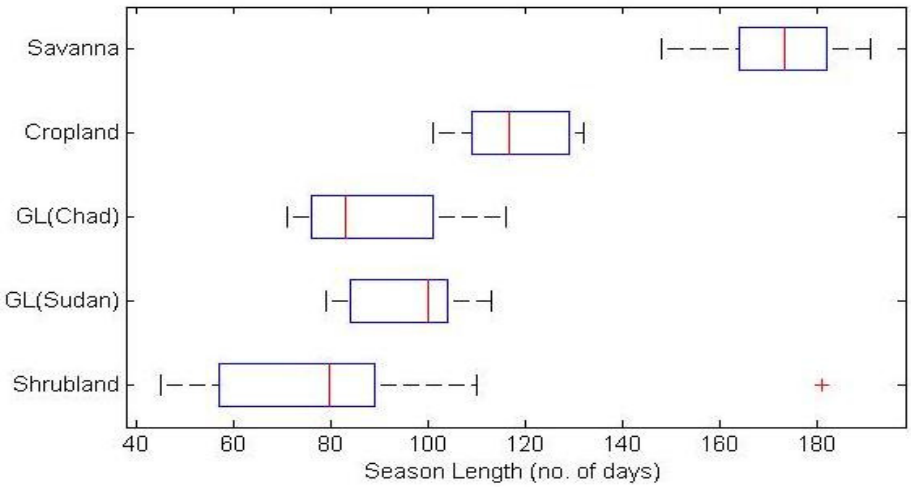

Figure 5.6: Boxplots showing the length of the growing season in different land cover classes during 2000-2009 (refer figure 5.1 caption for description).

Seasonal amplitude

The seasonal amplitude for each land cover is indicated in figure 5.7. Over the time period 2000-2009, an increase in shrubland, a steady condition in grassland (Sudan), a decrease in grassland (Chad), a steady condition in cropland and a decrease in savanna were observed. The statistical test outputs show that none was statistically significant (see appendix D).

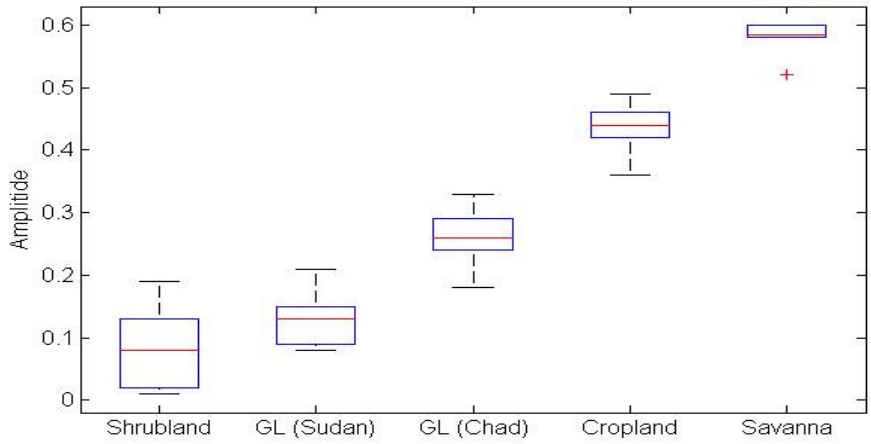

Figure 5.7: Boxplots showing seasonal amplitude in different land cover classes during 2000-2009 (refer figure 5.1 caption for description).

Small integral

The small integral for each land cover is indicated in figure 5.8. Over the time period 2000-2009, an increase in shrubland, and a decrease in all other land cover classes were observed and none was statistically significant (see appendix D).

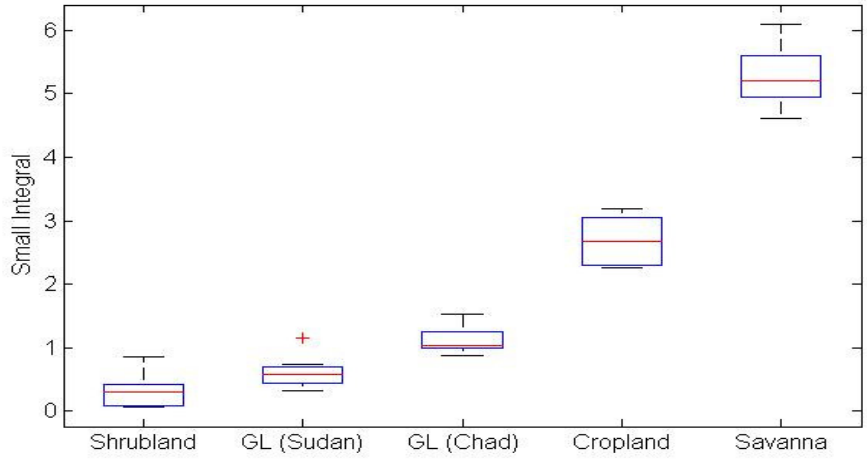

Figure 5.8: Boxplots showing the small integral in different land cover classes during 2000-2009 (refer figure 5.1 caption for description).

Large integral

The large integral for each land cover is indicated in figure 5.9. Over the time period 2000-2009, an increase was observed in shrubland and savanna while a decrease was observed in the grasslands and cropland. The statistical test outputs indicate that none was statistically significant (see appendix D).

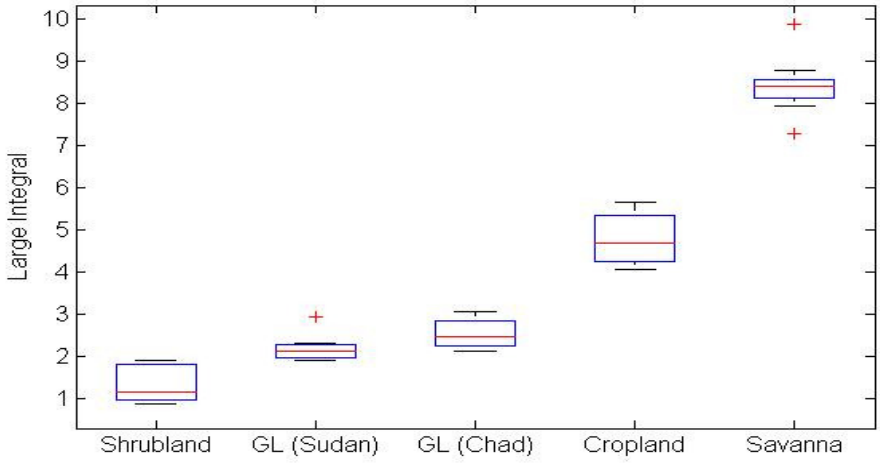

Figure 5.9: Boxplots showing the large integral in different land cover classes during 2000-2009 (refer figure 5.1 caption for description).

5.2. Spatial variation in NDVI (2000-2009)

A comparison of spatial variation over 2000-2009 based on class specific settings (as indicated in table 4.3) is presented for amplitude, length of the growing season and small integral. Figure 5.10 shows the seasonal amplitude during 2001, 2009 and the difference (2001 minus 2009) whereas figures 5.11 –5.13 depict the mean of the first half (2000-2004), second half (2005-2009) and the difference of the means.

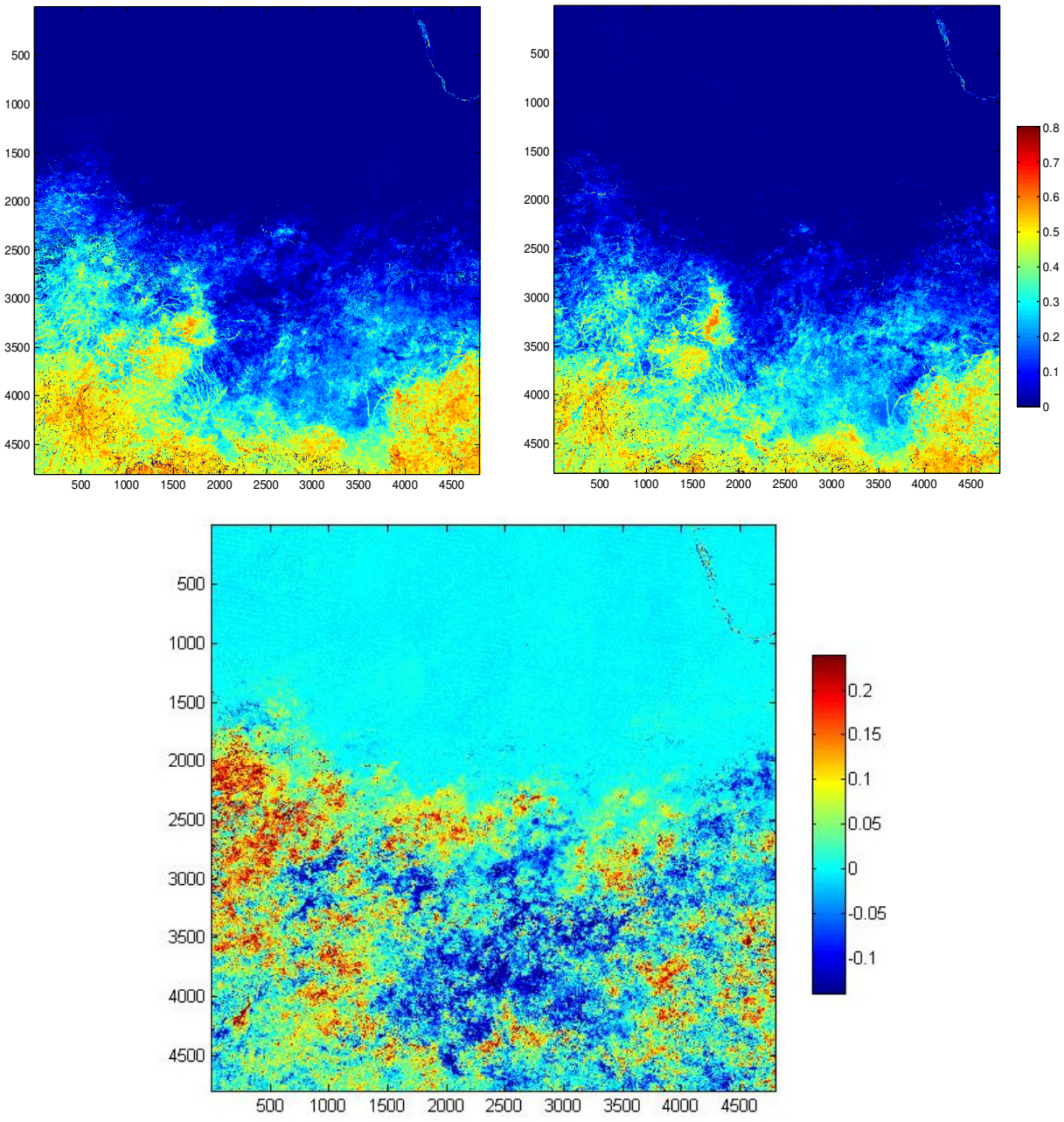

Figure 5.10: Seasonal amplitude for 2001 (top left), 2009 (top right), difference (2001-2009, bottom

The mean values of the second half of the time period (2005-2009) were deducted from the mean of the first half (2000-2004), i.e., mean (2000-2004) – mean (2005-2009). Hence, negative values indicate an increase and positive values indicate a decrease. Variations in amplitude and small integral were widely distributed (figures 5.10 - 5.12).
An increasing trend has been observed in the length of the growing season in the northern part and decreasing in the southern part (figure 5.13).
(N.B. The terms 'northern' and 'southern' are in reference to the image extent)

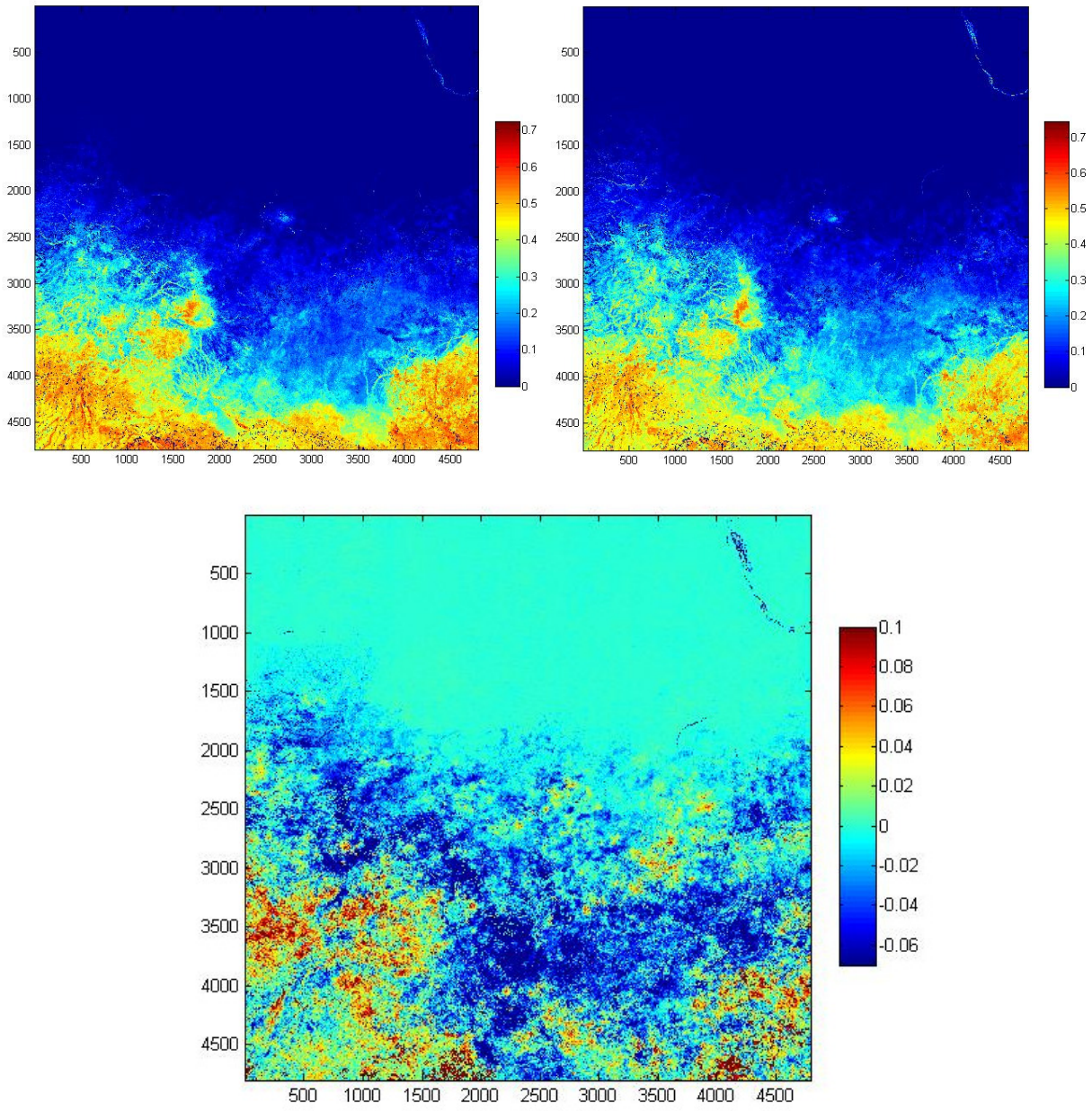

Figure 5.11: Seasonal amplitude mean1 (top left), mean2 (top right) and difference (mean1-mean2) (bottom). Mean1=2000-2004, and Mean2=2005-2009

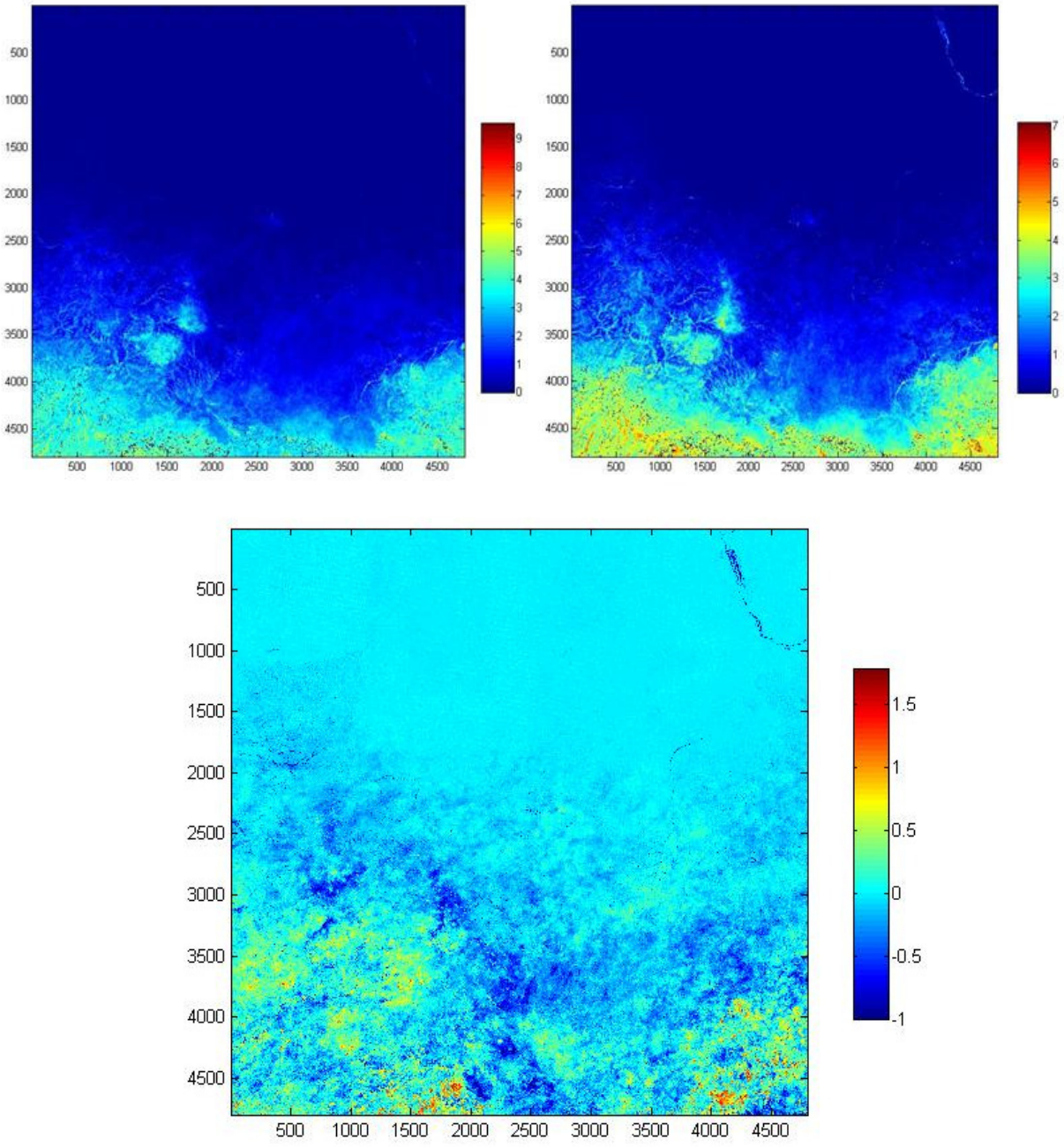

Figure 5.12: Small integral mean1 (top, left), mean2 (top, right) and difference (mean1-mean2) (bottom) Mean1=2000-2004, and Mean2=2005-2009

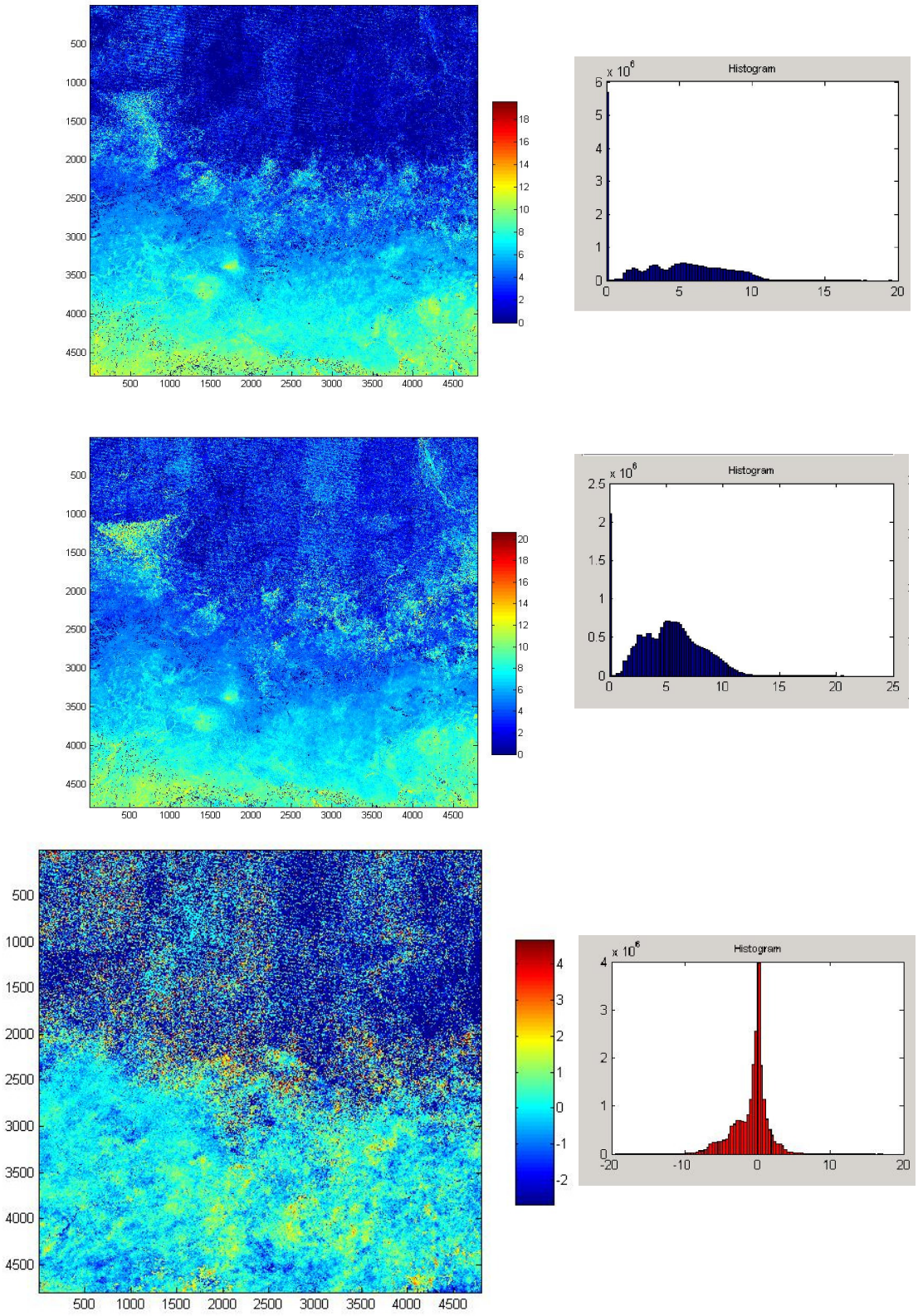

Figure 5.13: Length of the growing season and histograms: Season length mean1 (top), mean2 (middle) and difference (mean1-mean2) (bottom). Mean1=2000-2004, and Mean2=2005-2009

5.3. Rainfall (2001-2010)

Figure 5.14 (A-F) indicate the amount of rainfall for each land cover class, extracted for the sample sites and the observed changes were statistically non-significant (appendix D6).

A

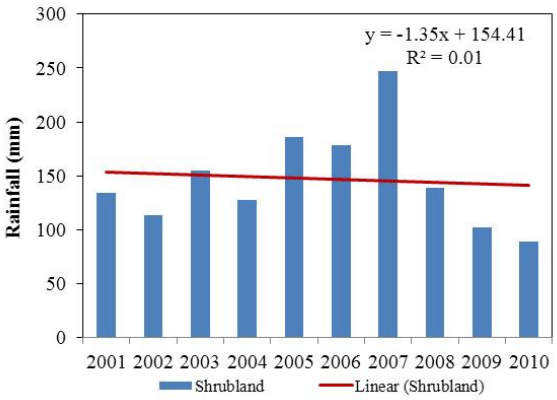

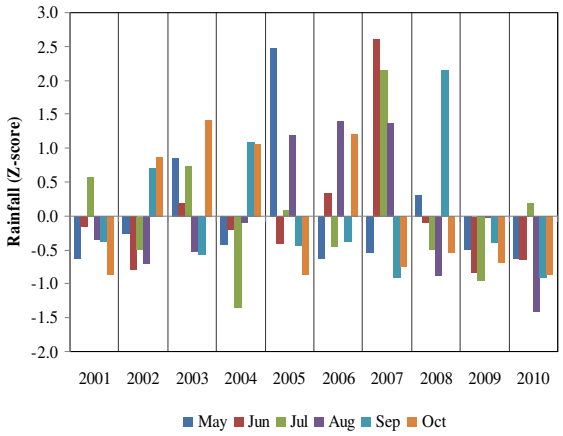

B

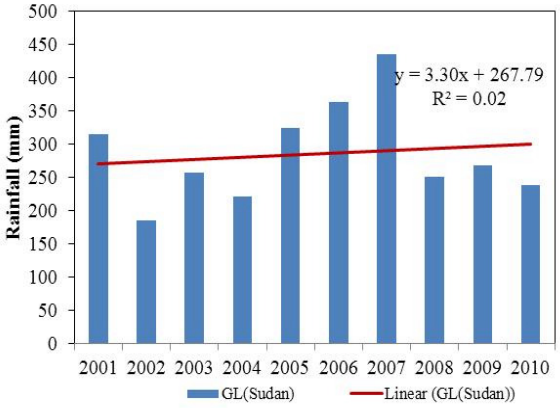

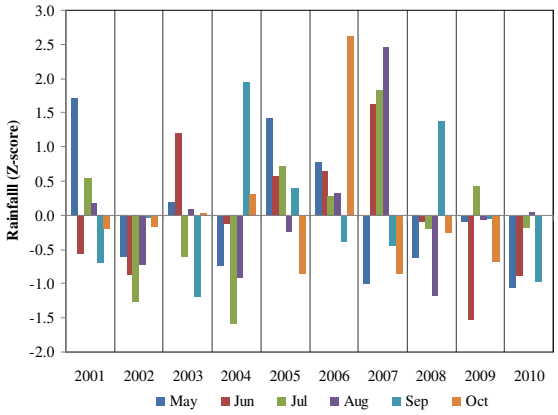

C

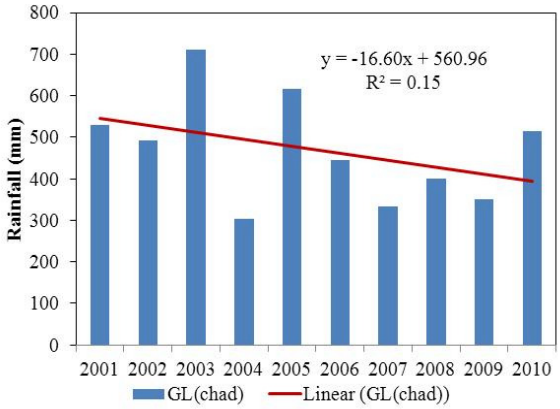

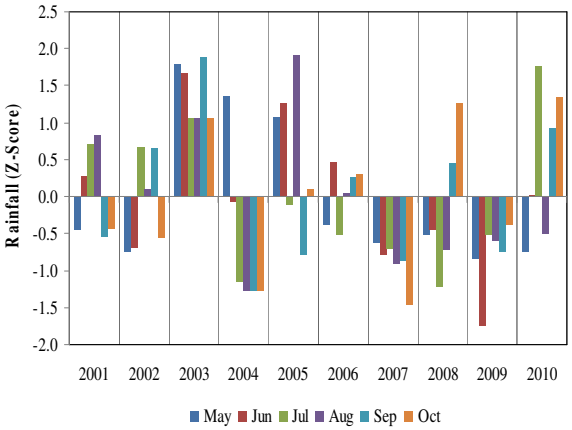

D

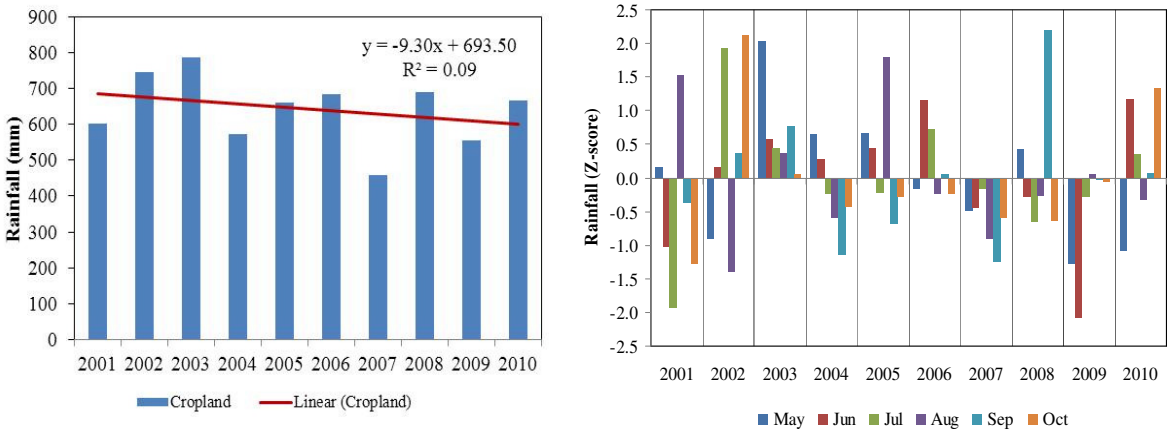

E

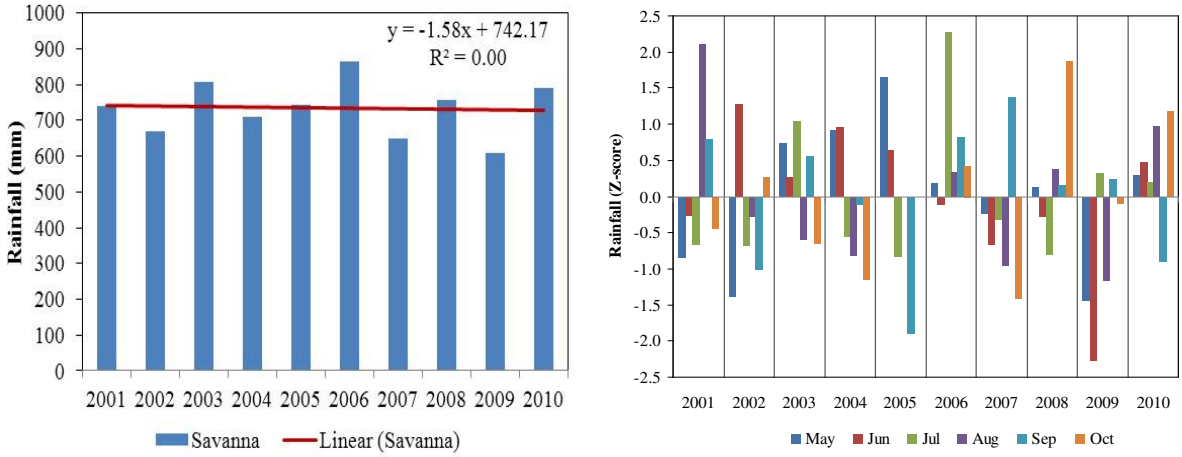

F

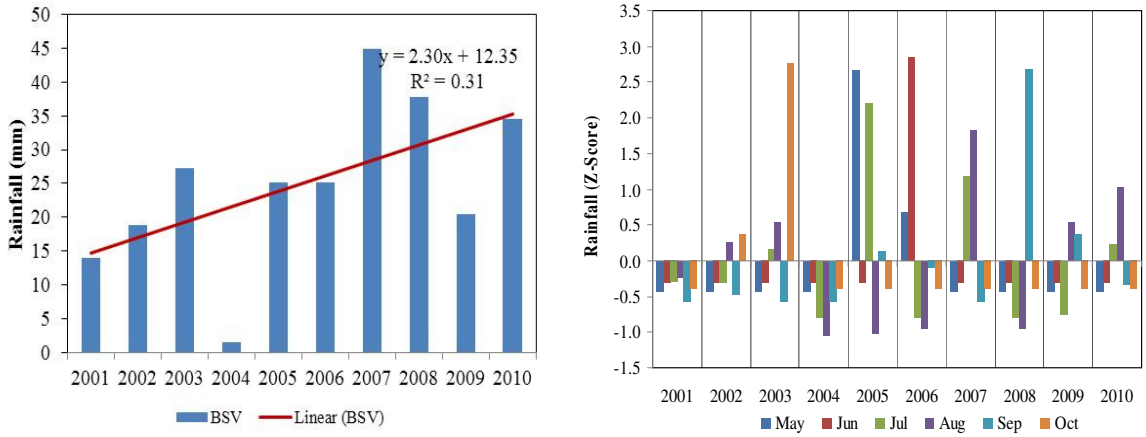

Figure 5 14: Rainfall over 2001-2010: annual values (left), rainy season z-score anomalies (right) for shrubland (A), grassland_Sudan (B), grassland_Chad (C), cropland (D), savanna (E) and barren or sparsely vegetated (F).

6. Discussion

6.1. NDVI temporal variation in different land cover classes

6.1.1. Shrubland

Shrubland is situated in the region, where according to Eklundh & Olsson (2003), a strong NDVI increase was observed during 1982-1999. In the current study, an increase in seasonal amplitude and integrals were marked over 2000-2009 and complements to the earlier increase reported by Eklundh & Olsson (2003). Significant increase in NDVI (figure 5.2A) was observed while a decrease in annual rainfall by about 15mm could be noted (figure 5.14A). The increase in NDVI despite the decrease in rainfall could be attributed to the influence of other factors and is in agreement with what Herrmann et al. (2005) has confirmed.

During 2001, high large integral was observed due to early start of the rainy season with sufficient amount (FAO report) (table 5.1 and appendix C1). Despite this fact, FAO reported poor harvest due to inconsistent distribution of rainfall and pest attacks. The low small integral value observed could, hence, be attributed to the poor harvest. This is in agreement with the report by Herrmann et al. (2005), who mentioned the likelihood of short-term impacts from pests in individual years. However, it is worth noting that the end of the growing season in 2001 is extended to January 2002 (table 5.1) and is not literal. The source of this error is from the dataset (figure 5.2A); missing seasonality of the first two seasons and causes discrepancy in the season length and other results.

Growing season length, amplitude and integrals were higher during 2002 than 2003, despite higher rainfall being recorded in 2003. This could partly be explained by rainfall distribution, since above normal rainfall amount has been recorded towards the end of the rainy season (Sep/Oct) during 2002 (fig 5.14A).
During 2007, exceptionally high amount of rainfall was the primary driver of the observed increase in amplitude and integrals. However, the length of the growing season is not consistent with the amount of rainfall observed. This could be related to the moisture available at root depth, since water logging and local flooding were marked due to excessive rainfall (www.fao.org/fileadmin/templates/tc/tce/pdf/Sudan_seasonal_monitor_Nov07.pdf).
This is consistent with the recent study by Jamali et al. (2011); Huber et al. (2011), who confirmed the relationship between rainfall and soil moisture to vegetation growth and the moisture available for plant growth depends on the soil type and root zone.

6.1.2. Grassland (Sudan)

Even though strong NDVI increase has been marked by Eklundh & Olsson (2003) in this region during 1982-1999, decreasing integrals and constant amplitude (appendix C2) was apparent during 2000-2009. A decrease in fitted NDVI (figure 5.2B) could also be noted despite the increase in annual rainfall (by about 30mm) observed over 2001-2010 (figure 5.14B). These findings are in agreement to that by Huber et al. (2011), who found a decreasing trend in central Sudan for the period 1982-2007. The decrease in integrals could be related to the decrease in the length of the growing season and high inter-annual variability.
During 2001 satisfactory amount and distribution of rainfall has been reported, as a result high growing season length and integrals were detected. Table 5.2 depicts similar season lengths for 2002, 2005 and 2007 but the integrals were higher during 2007. The high integrals

could be related to the high amount of rainfall recorded during 2007 (figure 5.14B). However, the highest season length would have been expected to follow the exceptionally high rainfall. The inconsistency of season length with the amount of rainfall could be explained by the effect of rainfall distribution and is consistent with the findings by Hielkema et al. (1986), who stated the possibility of NDVI being a good indicator of effective rainfall rather than total amount. Moreover, Ardö and Olsson (2003) underlined the importance of rainfall distribution in semi-arid regions, which are characterized by intense rainfall with few rain occurrences.

Despite the least (below normal) rainfall amount recoded in 2002, higher season length, amplitude and integrals have been observed relative to 2005 and could be related to the effect of rainfall distribution. Longer season length but lower amplitude, integrals and lower amount of rainfall were observed in 2004 compared to 2003 and 2008. These could indicate the influence of factors other than rainfall (such as, land management practices). This has been confirmed by Herrmann et al. (2005), who found spatially coherent trends in the residuals in their study of vegetation dynamics in the Sahel and related it to the possibility of other influencing factors.

6.1.3. Grassland (Chad)

This sample site also falls in the area of strong positive change marked by Eklundh & Olsson (2003). The fitted NDVI (figure 5.2C) showed an increase while a decline in annual rainfall was observed by about 150mm over 2001-2010 (figure 5.14C) and could be related to the effect of rainfall distribution. However, the amplitude and integrals were observed to decline despite the increase in the length of the growing season (see appendix C3). Apart from the high inter-annual variation, decreasing trend in integrals could be an indication of the increase in carbon sink in the Sahel discussed by Hickler et al., (2005) and Ardö et al., (2008).

The length and integrals being higher during 2003 compared to 2004, 2008, 2009 (table 5.3) could be related to the high amount of rainfall recorded in 2003 (figure 5.14C). Higher season length and integrals, but lower amount of rainfall in 2004 compared to 2008 and 2009 could be explained by the influence of rainfall distribution. Similar explanation could also be given to the higher integrals and season length, but lower rainfall amount observed during 2006 relative to 2002. These agree with the findings by Hielkema et al. (1986) and Ardö & Olsson (2003), who underlined the importance of rainfall distribution.

Higher large integral inconsistent with the small integral was observed in 2009 (relative to 2008) while the rainfall was below average. This could be attributed to the effect of non-photosynthetically active biomass. Even though the effect was localized, it could partly be explained by the above average biomass production reported due to early rains at the southern part of the country (http://www.fews.net/).
The longest growing season has been observed during 2007 despite the below normal amount of rainfall recorded. This could be attributed to other causative factors, such as pests and human effects, as has been stated by Herrmann et al. (2005). Besides, this region has been impacted by the migration of people to escape Darfur genocide (2003-2007), civil conflicts and consequent migrations (2005-2007). Hence, some of the vegetation changes could be attributed to such social setbacks and is consistent with the inferences made by Olsson (2008).

6.1.4. Cropland

The fitted NDVI (figure 5.2D) in this region shows an increase while annual rainfall has declined by about 90 mm over 2001-2010 (figure 5.14D). Cropland is situated in the region, where according to Eklundh & Olsson (2003), a strong increase was observed. Huber et al. (2011) and Heumann et al. (2007) have also recognized the region as 'hotspot' of maximum NDVI trend change. However, the findings of the current study were not complementary to the findings by the above-mentioned researchers. Steady condition of seasonal amplitude and a decrease in integrated NDVI were evident over 2000-2009 (appendix C4). One reason for the difference is the time span considered. Decline in the length of the growing season is another determining factor and is related to the observed decrease in rainfall amount. The constant amplitude could partly be explained by saturation property of NDVI and agrees to what Fensholt et al. (2009) have found in the croplands in the central and East Africa. Similarly, the study by Hickler et al. (2005) states that integrals are more appropriate indicators of changes in vegetation due to the saturation evident in seasonal amplitude at highly vegetated areas.

In addition, this region is under intensive farming and grazing conditions, which could impact the soil fertility negatively and subsequently, decrease vegetation production. The decrease in integrals from 2003-2004 and 2005-2006, for instance, could be due to the decrease in agricultural production reported by FAO. Although the decrease in rainfall from 2003-2004 has an impact, higher amount of annual rainfall was recorded during 2006 (figure 5.14D). Besides, the genocide in Darfur (2003-2007) has unavoidable effects to the vegetation observed during 2003-2004 and 2005-2006.

Even though the same amplitudes were observed during 2002, 2005 and 2008 (table 5.4), the integrals were higher during 2008. As it is indicated in fig 5.14D, however, higher rainfall was recorded during 2002. Similarly, longest season length and highest large integral was observed during 2001, while the annual rainfall was below average. In line with this, despite the lowest amount of rainfall recorded and short length of the growing season observed (table 5.4), above average amplitude was observed during 2007. Taking the fact that integrals are responsive to extended growing seasons unlike amplitude, which could be influenced by short season, the distribution of rainfall is also an important controlling factor. This is also consistent with the findings by Hielkema et al. (1986) and Ardö and Olsson (2003).

Overall, the NDVI was not totally dependent on the amount of rainfall. Other factors such as intensity and distribution of rainfall, irrigation activities, pests, land management practices, crop rotation, harvesting and fire also impact the NDVI signals captured over time. In addition, migrations due to civil conflicts and land use management practices have an influence on the vegetation and this is in agreement to the discussions given by Olsson (2008).

6.1.5. Savanna

Savanna is located in the region of strong NDVI increase reported by Eklundh & Olsson (2003). The fitted NDVI in the current study was observed to increase (figure 5.2E) while a slight decline in annual rainfall was observed over 2001-2010 (figure 5.14E). The results are not complementary to the findings by Eklundh & Olsson (2003). A decrease in amplitude and small integral were observed over 2000-2009 despite an increase in the length of the growing season (see appendix C5). This could be influenced by the high inter-annual variation and be

indication of the increase in carbon sink in the Sahel discussed by Hickler et al. (2005) and Ardö et al. (2008).

The highest amount of rainfall was recorded during 2006 (figure 5.14E), however the longest growing season and the highest integrals were observed during 2003 (table 5.5). Similarly, longer season length and higher integrals were observed during 2007 compared to 2001 while the amount of rainfall in 2007 was below average, but not for 2001. These could be related to the effect of rainfall distribution similar to the other land cover classes (Hielkema et al., 1986; Ardö and Olsson, 2003).

Higher season length and integrals during 2005 relative to 2002 could be attributed to the relatively higher rainfall amount. Late start of rainfall followed by below average amount was reported during 2002 and led to short season length and integrals. Similarly, the longest season was observed in 2008 accompanied by slightly above normal rainfall. But the small integral was below average and could partly be an indication of other causative factors as stated by Hielkema et al. (1986); Ardö and Olsson (2003); Herrmann et al. (2005). The above facts could also be explained by the effect of rainfall being less in humid areas. This conforms to the findings by Fensholt and Rasmussen (2011), who found inconsistent relationship between rainfall and NDVI during 1996-2007 in the region with mean annual precipitation greater than 700mm.
Besides, low integrals during 2001, 2002, 2007-2009 could be related to low primary production. This is in agreement with what Ardö and Olsson (2003) have reported in that the seasonal variation in water availability influences NPP in semi-arid areas.

In general the delay on the onset of the growing seasons, which cause decline in the season length, was due to late start of rainfall, even if an increase in the amount of rainfall was observed. This agrees to the recent finding by Simon and Laura (2011), who found significant negative impact of the number of dry days upon vegetation. Previous other studies (D'Amato and Lebel, 1998; Le Barbe´ and Lebel, 1997) have reported that a decrease in the number of rain occurrences is the major cause of the decline in precipitation observed during 1970–1989 in the central Sahel.

6.2. Spatial variation in NDVI

The results from the current study indicate spatial variation in NDVI and phenological parameters. The amplitudes and small integral (figures 5.10-5.12) were consistent with the findings by Heumann et al. (2007) who found significant trends in amplitude and small integral in the Sahel. However, the result of the length did not conform to the findings by Heumann et al., who analysed data of 1982-2005 and did not take into account the pattern after 2005. Besides, the difference in the results could arise from the datasets used (MODIS-NDVI vs. GIMMS-NDVI), composite days (16day vs. 10day) and TIMESAT fitting functions chosen. Fensholt et al. (2009), for instance, mentioned the effect of the length of compositing periods on time of the growing season and integrals.
The variation, in general, is related to the inherent disparity in climate, land cover, vegetation type, land management practices and topography. The type of soil underlying each land cover could also be one of the factors influencing the spatial variation since it is an intrinsic characteristic to soil water holding capacity or moisture availability. These agree with the findings by Zhang et al. (2005); Jamali et al. (2011); Huber et al. (2011). Other potential cause could be the response of each land cover to imposed actions. For instance, Ardö and Olsson (2003) have studied the effect of grazing on soil organic carbon in grassland and Savanna of Sudan. Their study reveals opposite conditions in savanna and grasslands under similar grazing patterns, which they attributed it to the difference in the amount of rainfall.

The spatial variation in NDVI is also a factor of the species composition (percentage of annuals and perennials) and adaptation mechanism of the land cover classes to drought conditions. As indicated in table 2.2, for instance, savanna has 10 – 60 % tree canopy cover with relatively deep roots unlike those in the northern and central parts in the Sahel (Huber et al., 2011). The tree canopies provide shade that decreases the evaporation from the soil. Hence, there will be less response to variable rainfall conditions. This is consistent with the recent findings by Fensholt and Rasmussen (2011) and Simon and Laura (2011). Fensholt and Rasmussen noted less correlation between NDVI and rainfall in the southern part of the Sahel and attributed it to factors other than rainfall. The study by Simon and Laura (2011) noted the difference in growth trends in different land cover classes in the Sahel. Their study reveals larger negative correlation between length of dry periods after start of the rainy season and NDVI in grassland and shrubland than in the cropland.

On the other hand, regions with less canopy cover have low moisture status during the dry season and seasonal NDVI variation could be evident (Heumann et al., 2007). Besides, NDVI signals in shrubland could be affected by soil background effects as the vegetation cover is sparse and failure of MVC technique to handle such conditions (details given in section 3.2.3). Barren or sparsely vegetated land cover (desert region) did not show any change in amplitude and integral over time (figure 5.10-5.12), as expected. This is in agreement with Fensholt et al. (2009)'s findings. However, an increase in the season length (figure 5.13) was observed, which could be related to the increase in the amount of rainfall (figure 5.14F) and/or change in dominant species observed during the time period

Moreover, agriculture-related activities (from land preparation to harvesting, including irrigation) have considerable impacts on vegetation (Eklundh, 1996). Furthermore, changes in land use, short-term impacts from pests or diseases, population and grazing pressures and civil conflicts are other causative factors (Eklundh and Olsson, 2003; Olsson et al., 2005; Herrmann et al., 2005; Olsson, 2008; Fensholt and Rasmussen, 2011).

6.3. Discussion summary

The evaluation of the hypotheses defined in section 1.2 is presented below.

$H_0$1 Temporal changes in NDVI and phenological parameters were not evident within each land cover during 2000-2010.

The results from the current study reveal high temporal (between-year and within year) variations in NDVI and phenological parameters in each land cover class (tables 5.1-5.5 and appendix C). These conform to the high seasonal variation in vegetation in this region and agree to the findings by Fensholt and Rasmussen (2011). Besides several researchers: Ardö and Olsson (2003); Seaquist et al. (2005); Herrmann et al. (2005); Zhang et al., 2005; Ardö et al., 2008; Simon and Laura (2011), being amongst the few, have witnessed the temporal NDVI variation in this region. "Arid environments are seen as highly variable 'event-driven' rather than equilibrium systems; disturbed or degraded by human impact" (Rasmussen et al., 2001, pp., 281). In this case, the assumption of the null hypothesis is not met and it can be rejected.
However, the statistical test outputs (appendix D) reveal that most of the observed changes were not significant. One of the causes for the insignificance of the statistical tests could be the effect of the sample size as the likelihood of obtaining erroneous results is largely associated with smaller sample sizes.

Conclusion: Temporal changes in NDVI and phenological parameters were evident within each land cover during 2000-2010 but cannot be statistically confirmed.

$H_0$2 Spatial variations in phenological parameters were not evident during 2000-2009.

The analysis outputs revealed spatial variations in NDVI and phenological parameters (amplitude, integrals and length of the growing season) as presented in figures 5.10-5.13. This agrees largely to the findings by Olsson et al., 2005; Anyamba & Tucker, 2005; Zhang et al., 2005; Fensholt et al., 2009; Huber et al., 2011; Fensholt and Rasmussen, 2011; Simon and Laura (2011). In this case, the assumption of the null hypothesis is not met and it can be rejected.
On the other hand, as stated earlier, the statistical test outputs (appendix D) reveal insignificance for most of the cases.

Conclusion: It is dubious to draw conclusions on the spatial variations in phenological parameters and further inspection with larger sample sizes is recommended.

$H_0$3 The amount of rainfall was not the main driving factor for the observed changes in NDVI and phenological parameters during 2000-2010.

The results indicate that the increase in rainfall amount did not necessarily cause an increase in NDVI or vice versa. This indicates that amount of rainfall was not the only factor affecting the vegetation during 2000-2010. This agrees with the results presented by Olsson et al. (2005), who discovered a positive, but unreliable relationship between vegetation and rainfall patterns. Moreover, Eklundh and Sjöström (2009) mentioned that the observed greening could not only be explained by an increase in rainfall. This has also been confirmed by Huber et al. (2011), who found out that NDVI responds only partly to the increase in rainfall and soil moisture observed from west to east across Sahel during 1982-2007. Furthermore, the

study by Simon and Laura (2011) reveals the importance of inter-annual variation in rainfall (the number of rainy days) not the amount. Fensholt and Rasmussen (2011) stated changes in vegetation could not be explained by rainfall alone, other factors such as: rain-use efficiency and anthropogenic effects should also be considered.
The assumption of the null hypothesis is met and hence, it cannot be rejected.

Conclusion: The amount of rainfall was not the main driving factor for the observed changes in NDVI and phenological parameters during 2000-2010.

7. Sources of uncertainty

- For stratification, the land cover product of 2004 was used, which does not represent the conditions before and after. In addition, it is likely that the land cover classes were not stable over the time period. This could be due to replacement of the natural vegetation with cultivated fields, in which agriculture-related activities (from land preparation to harvesting including fallow periods) have profound effects on vegetation cover.

- Effects from clouds, since weights have not been implemented. Eklundh and Jönsson (2009) stated that cloudy conditions amplify the negative bias in the noise.

- Uncertainty from MVC NDVI, which is subject to both atmospheric and anisotropic (bi-directional) properties (details given in section 3.2.3).

- Uncertainties from TIMESAT assumptions (section 3.3.2) and smoothing functions employed as the performance of the smoothing functions is greatly influenced by the strength and source of the noise in the dataset.

- The threshold values given for start and end of the growing seasons. Particularly, the values given for the season end seem to be high (table 4.3) to minimize the effects of dry biomass: and lesser values could lead to end of the growing seasons being extended to the following years.

- Due to the high inter-annual variation, the settings in TIMESAT fit well for some years but not for others. For instance, the end of the growing seasons in shrubland during 2001 and in savanna during 2007 and 2009 are observed in January of the following years.

- Uncertainties from the rainfall data and relating it to NDVI of different spatial resolution. The rainfall grids have 0.1-degree (10km) resolution and NDVI 5x250m (1.25km). Besides, monthly rainfall is computed for each land cover and does not match with the 16day composite NDVI images. It could only give a rough estimate of the effect of rainfall on NDVI. Therefore, the conclusions drawn based on NDVI/rainfall relationships might be intuitive assumptions.

- Discrepancies arising from averaging different seasons/years since there are high seasonal fluctuations.

8. Conclusion

In this study, assessments of the spatial and temporal variation in NDVI and phenological parameters were made for parts of the Sudan and Chad. The findings were explained by looking at the potential effect of the amount of rainfall and are summarized below.

- The results revealed high temporal variations in NDVI and phenological parameters in each land cover class. Besides, spatial variations in phenological parameters were evident.
- The temporal and spatial variations observed could not be confirmed statistically, possibly due to small sample size. Hence, further inspection with larger sample sizes is recommended.
- The findings reveal that observed changes could not be explained by the amount of rainfall alone.
- In most cases, the observed increase in integrals is related to increase in length of the growing season. However, despite the likelihood that higher amplitude would be related to longer season length (has also been confirmed by Heumann et al., 2007), a negative relationship has been observed. This is in agreement with what Heumann et al. (2007) found for Soudanian and Guinean regions, not for the Sahel and further inspection is recommended.
- The time period 2000-2010 is short for making inferences, hence extended time period is recommended for robustness of the results. This is in agreement with the report by Fensholt and Rasmussen (2011), who pointed out the significance of consistent trends being masked when inadequate number of years is considered.
- Phenology is temperature dependent. Even though the major factor in arid and semi-arid regions is availability of water, precise outputs could be achieved by including such determinant factors. This has also been confirmed by Héllden and Tottrup (2008).
- Comparison of findings of the current study with other previous studies might not be straightforward. Differences could arise due to analyzed time periods, study area, composite days, data from different sensors and approaches of analysis. This agrees to the statements given by Ardö et al., 2008; Eklundh and Sjöström, 2009; Fensholt et al., 2009.
- Overall, the findings from this study are unpredictable. In some cases the fitted NDVI was observed to increase while the seasonality parameter outputs (amplitude, small integral and season length) were decreasing. These inconsistencies make the attribution of the possible reasons complicated. Better explanation of the situation could be achieved by considering other factors, which influence vegetation. Land management practices, land use changes, temperature (in relation to NPP), rainfall intensity and distribution, soil type, and human influences over extended time periods are amongst the few. This agrees with previous inferences made. The greening trend in the Sahel remains under discussion (Huber et al., 2011), the direction of change and its underlying causes are not known yet and better explanation could be achieved by looking into other causative factors (Herrmann et al., 2005; Héllden and Tottrup, 2008).

Future perspectives to TIMESAT

This study emphasizes the efficiency of TIMESAT and looks forward to future improvements to handle inter-annual variability.

9. References

Agnew C.T., Chappell A. (1999) Drought in the Sahel. GeoJournal 48:299-311.

Anyamba A., Tucker C.J. (2005) Analysis of Sahelian vegetation dynamics using NOAA-AVHRR NDVI data from 1981-2003. Journal of Arid Environments 63:596-614.

Ardö J., Mölder M., El-Tahir B., Elkhidir H. (2008) Seasonal variation of carbon fluxes in a sparse savanna in semi-arid Sudan. Carbon Balance and Management 3:7.

Ardö J., Olsson L. (2003) Assessment of soil organic carbon in semi-arid Sudan using GIS and the CENTURY model. Journal of Arid Environments 54:633-651.

Badeck, F.W., Bondeau, A., Böttcher, K., Doktor, D., Lucht, W., Schaber, J. and Sitch, S. (2004) Responses of spring phenology to climate change. New Phytologist, 162: 295–309.

Beck P.S.A., Atzberger C., Hogda K.A., Johansen B., Skidmore A.K. (2006) Improved monitoring of vegetation dynamics at very high latitudes: A new method using MODIS NDVI. Remote Sensing of Environment 100:321-334.

Canadell J., Noble I. (2001) Challenges of a changing Earth. Trends in Ecology and Evolution 16:664-666.

Chappell, Seaquist, Eklundh. (2001) Improving the estimation of noise from NOAA AVHRR NDVI for Africa using geostatistics. International journal of remote sensing 22:1067-1080.

Chen J., Jonsson P., Tamura M., Gu Z., Matsushita B., Eklundh L. (2004) A simple method for reconstructing a high-quality NDVI time-series data set based on the Savitzky-Golay filter. Remote Sensing of Environment 91:332-344.

Cihlar J., Manak D., Voisin N. (1994) AVHRR bidirectional reflectance effects and compositing. Remote Sensing of Environment 48:77-88.

Cihlar J., Manak D., amp, apos, Iorio M. (1994) Evaluation of compositing algorithms for AVHRR data over land. Geoscience and Remote Sensing, IEEE Transactions on 32:427-437.

Cihlar, J., Ly, H., Li, Z., Chen, J., Pokrant, H., & Huang, F. (1997) Multitemporal, multichannel AVHRR data sets for land biosphere studies: artifacts and corrections. Remote Sensing of Environment, 60:35–57.

D'Amato N. and Lebel T., (1998) On the characteristics of the rainfall events in the Sahel with a view to the analysis of climatic variability. International Journal of Climatology 18:955–974.

Defries R.S., Hansen M.C., Townshend J.R.G. (2000) Global continuous fields of vegetation characteristics: A linear mixture model applied to multi-year 8 km AVHRR data. International journal of remote sensing 21:1389-1414.

Dregne H.E. (1986) Desertification of arid lands. In El-Baz, F. and Hassan, M. H. A. (ed.). Physics of desertification. Dordrecht, Netherlands : Martinus, Nijhoff.

Eklundh, Lars (1996) AVHRR NDVI for monitoring and mapping of vegetation and drought in East African environments. Dissertation. Lund University.

Eklundh, L., and Olsson L., (2003) Vegetation index trends for the African Sahel 1982–1999. Geophysical Research Letters. 30(8), 1430.

Eklundh, L. and Jönsson, P., 2009, Timesat 3.0 Software Manual. Lund University, Sweden.

Eklundh L., Sjöström M. (2005) Analysing vegetation changes in the Sahel using sensor data from Landsat and NOAA. 31st International Symposium on Remote Sensing of Environment

El Nadi, Abdel Mohsin (2005) Preliminary estimates of potential evapotranspiration, rainfall and crop water requirement in the Sudan: A signal for water shortage in future. Faculty of Agriculture University of Khartoum, Sudan

Eltahir EAB (1996) Role of vegetation in sustaining large-scale atmospheric circulation in the tropics. Journal of Geophysical Research 101:4255-4268

Fensholt R. (2004) Earth observation of vegetation status in the Sahelian and Sudanian West Africa: comparison of Terra MODIS and NOAA AVHRR satellite data. International Journal of Remote Sensing 25:1641-1659.

Fensholt R., Sandholt I., Rasmussen M.S. (2004) Evaluation of MODIS LAI, fAPAR and the relation between fAPAR and NDVI in a semi-arid environment using in situ measurements. Remote Sensing of Environment 91:490-507.

Fensholt R., Sandholt I. (2005) Evaluation of MODIS and NOAA AVHRR vegetation indices with in situ measurements in a semi-arid environment. International Journal of Remote Sensing 26:2561-2594.

Fensholt R., Sandholt I., Rasmussen M.S., Stisen S., Diouf A. (2006) Evaluation of satellite based primary production modelling in the semi-arid Sahel. Remote Sensing of Environment 105:173-188.

Fensholt R., Rasmussen K., Nielsen T.T., Mbow C. (2009) Evaluation of earth observation based long-term vegetation trends - Intercomparing NDVI time series trend analysis consistency of Sahel from AVHRR GIMMS, Terra MODIS and SPOT VGT data. Remote Sensing of Environment 113:1886-1898.

Fensholt R., Rasmussen K. (2011) Analysis of trends in the Sahelian 'rain-use efficiency' using GIMMS NDVI, RFE and GPCP rainfall data. Remote Sensing of Environment 115:438-451.

Friedl M.A., McIver D.K., Hodges J.C.F., Zhang X.Y., Muchoney D., Strahler A.H., Woodcock C.E., Gopal S., Schneider A., Cooper A., Baccini A., Gao F., Schaaf C. (2002) Global land cover mapping from MODIS: algorithms and early results. Remote Sensing of Environment 83:287-302.

Giannini A., Saravanan R., Chang P. (2003) Oceanic Forcing of Sahel Rainfall on Interannual to Interdecadal Time Scales. Science 302:1027-1030.

Gitas, I., Mitri, G., Avyikou, I. & Diamanti, E. (2004) Vegetation greenness mapping of Greece using MODIS imagery. Workshop on MODIS Data and Imagery: Valladolid, Spain, June 24–25.

Goward, S., Markham, B., & Dye, D. (1991) Normalized difference vegetation index measurements from the advanced very high resolution radiometer. Remote Sensing of Environment 35:257–277.

Guyot, G., Gugon, D., & Riom, J. (1989) Factors affecting the spectral response of forest canopies: A review. Geocarta International 3: 43–60.

Hare F.K., (1984) Climate, drought and desertification. Nature and Resources UNESCO 20:2-8

Héllden U., Tottrup C. (2008) Regional desertification: A global synthesis. Global and Planetary Change 64:169-176.

Herrmann S.M., Anyamba A., Tucker C.J. (2005) Recent trends in vegetation dynamics in the African Sahel and their relationship to climate. Global Environmental Change 15:394-404.

Heumann B.W., Seaquist J.W., Eklundh L., Jonsson P. (2007) AVHRR derived phenological change in the Sahel and Soudan, Africa, 1982-2005. Remote Sensing of Environment 108:385-392.

Hickler T., Eklundh L., Seaquist J.W., Smith B., Ardö J., Olsoon L., Sykes M.T., and Sjostrom M. (2005) Precipitation controls Sahel greening trend. Geophysical Research Letters 32: L21415

Hielkema J.U., Prince S.D., Astle W.L. (1986) Rainfall and vegetation monitoring in the Savanna Zone of the Democratic Republic of Sudan using the NOAA Advanced Very High Resolution Radiometer. International Journal of Remote Sensing 7:1499-1513.

Hird J.N., McDermid G.J. (2009) Noise reduction of NDVI time series: An empirical comparison of selected techniques. Remote Sensing of Environment 113:248-258.

Holben, B. (1986) Characteristics of maximum-value composite images from temporal AVHRR data. International Journal of Remote Sensing 7: 1417−1434.

Houerou H.N.L. (1980) The Rangelands of the Sahel. Journal of Range Management 33:41-46.

Huber S., Fensholt R., Rasmussen K. (2011) Water availability as the driver of vegetation dynamics in the African Sahel from 1982 to 2007. Global and Planetary Change 76:186-195.

Huete A.R., Jackson R.D. (1988) Soil and atmosphere influences on the spectra of partial canopies. Remote Sensing of Environment 25:89-105.

Huete, A., Justice, C., & van Leeuwen (1999). MODIS Vegetation Index (MOD13) Algorithm Theoretical Basis Document, Version 3.

Huete A., Didan K., Miura T., Rodriguez E.P., Gao X., Ferreira L.G. (2002) Overview of the radiometric and biophysical performance of the MODIS vegetation indices. Remote Sensing of Environment 83:195-213.

Hyman A. H. and Barnsley M. J. (1997) On the potential for land cover mapping from multiple-view-angle (MVA) remotely sensed images. International Journal of Remote Sensing 18:2471–2475.

Jackson R.D., Slater P.N., Pinter P.J. (1983) Discrimination of growth and water stress in wheat by various vegetation indices through clear and turbid atmospheres. Remote Sensing of Environment 13:187-208.

Jamali, S., Seaquist, J., Ardö, J., Eklundh, L., (2011) Investigating temporal relationships between rainfall, soil moisture and MODIS-derived NDVI and EVI for six sites in Africa. 34th International Symposium on Remote Sensing of Environment, Sydney Convention and Exhibition Centre, Australia.

Jones, K.B., Ritters, K.H., Wickham, J.D., Tankersley, R.D. O'Neill, R.V., Chaloud, D.J., Smith, E.R. & Neale, A.C. (1998) An Ecological assessment of the United States: Mid-Atlantic Region, Washington: EPA, p. 103.

Jönsson A.M., Eklundh L., Hellstrom M., Barring L., Jonsson P. (2010) Annual changes in MODIS vegetation indices of Swedish coniferous forests in relation to snow dynamics and tree phenology. Remote Sensing of Environment 114:2719-2730.

Jönsson P., Eklundh L. (2002) Seasonality extraction and noise removal by function fitting to time-series of satellite sensor data. Geoscience and Remote Sensing, IEEE Transactions 40:1824-1832.

Jönsson P., Eklundh L. (2004) TIMESAT-a program for analyzing time-series of satellite sensor data. Computers and Geosciences 30:833-845.

Justice C.O., Hiernaux P.H.Y. (1986) Monitoring the grasslands of the Sahel using NOAA AVHRR data: Niger 1983. International Journal of Remote Sensing 7:1475-1497.

Katagis, T, Gitas, I., Alexandridis, T., Topaloglou, C. & Silleos, N. (2006). Developing MODIS time series for monitoring vegetation condition: preliminary results. Proceedings of 26th Symposium of European Association of Remote Sensing Laboratories (EARSeL), 29 May – 2 June, Warsaw, Poland.

Lamb H.H., (1974) The Earth's changing climate. Ecologist 4:10–15.

Le Barbé, L. and Lebel, T. (1997) Rainfall climatology of the HAPEX-Sahel region during the years 1950–1990. Journal of Hydrology 188–189:43–73.
Maselli F. (2004) Monitoring forest conditions in a protected Mediterranean coastal area by the analysis of multiyear NDVI data. Remote Sensing of Environment 89:423-433.
Rautiainen, M., Heiskanena, J., Eklundh, L., Mõttusc, M., Lukeš, P., Stenberg, P. (2010) Ecological applications of physically based remote sensing methods. Scandinavian Journal of Forest Research 25:325-339.
Monteith J.L. (1972) Solar Radiation and Productivity in Tropical Ecosystems. Journal of Applied Ecology 9:747-766.
Moody A., Strahler A.H. (1994) Characteristics of composited AVHRR data and problems in their classification. International journal of remote sensing 15:3473-3491.
Nicholson, S.E., Tucker, C.J. & Ba, M.B. (1998) Desertification, drought and surface vegetation: an example from the West African Sahel. Bulletin of the American Meteorological Society 79: 815–829.
Ning Z., Neelin J.D., Lau K.M., Compton J.T. (1999) Enhancement of Interdecadal Climate Variability in the Sahel by Vegetation Interaction. Science 286:1537-1540.
Olsson L., (1993) Desertification in Africa - Critique and an Alternative Approach. GeoJournal 31:23-32
Olsson L., (1993) On the Causes of Famine: Drought, Desertification and Market Failure in the Sudan. Ambio 22:395-403.
Olsson L., Eklundh L., Ardö J. (2005) A recent greening of the Sahel-trends, patterns and potential causes. Journal of Arid Environments 63:556-566.
Olsson, L. (Lead Author) and Hall-Beyer, M (Topic Editor) (2008) Greening of the Sahel. Encyclopedia of Earth. Eds. Cutler J. Cleveland (Washington, D.C.: Environmental Information Coalition, National Council for Science and the Environment).
Prince, S., and Coauthors (1995) Geographical, biological and remote sensing aspects of the Hydrologic Atmospheric Pilot Experiment in the Sahel (HAPEX-Sahel). Remote Sensing of Environment 51:215–234.
Rasmussen K., Fog B., Madsen J.E. (2001) Desertification in reverse? Observations from northern Burkina Faso. Global Environmental Change 11:271-282.
Reynolds J.F., Smith D.M.S., Lennart O. (2004) Global Desertification: Do Humans Cause Deserts? Geographical Review 93:413-415.
Salim H.Z., X. Chen and J. Gong, (2008) Analysis of Sudan vegetation dynamics using NOAA-AVHRR NDVI data from 1982-1993. Asian Journal of Earth Sciences 1:1-15.
Seaquist, J., (2001) Mapping primary production for the West African Sahel with satellite data. Meddelanden från Lunds Universitets Geografiska Instutitioner, Avhandlingar 140.
Seaquist J.W., Olsson L., Ardö J. (2003) A remote sensing-based primary production model for grassland biomes. Ecological Modelling 169:131-155.
Simon Richard P., Laura Vang R. (2011) The influence of seasonal rainfall upon Sahel vegetation. Remote Sensing Letters 2:241-249.
Sjöström, M. (2004) Investigating vegetation changes in the African Sahel 1982-2002: a comparative analysis using Landsat, MODIS and AVHRR remote sensing data. Seminar series nr.106, Geobiosphere Science Center, Lund University, Sweden. pp71.
Sjöström M., Ardö J., Eklundh L., El-Tahir B.A., El-Khidir H.A.M., Hellström M., Pilesjö P., Seaquist J. (2009) Evaluation of satellite based indices for gross primary production estimates in a sparse savanna in the Sudan. Biogeosciences 6:129-138.
Strahler, A., Muchoney, D., Borak, J., Friedl, M., Gopal, S., Moody, A., and Lambin, E., (1999) MODIS Land Cover Product Algorithm Theoretical Basis Document (ATBD), Version 5.0 (Boston: Boston University).

Tooze S., (1984): Sahel drought, call for joint action. Nature 307:497.
Townshend, J. R. G., C. Justice, W. Li, C. Gurney, and J. McManus, (1991) Global land cover classification by remote sensing: Present capabilities and future possibilities. Remote Sensing of Environment 35:243–255.
Tucker C.J., Vanpraet C.L., Sharman M.J., Van Ittersum G. (1985) Satellite remote sensing of total herbaceous biomass production in the senegalese sahel: 1980-1984. Remote Sensing of Environment 17:233-249.
Tucker, C. J., & Nicholson, S. E. (1999) Variations in the size of the Sahara Desert from 1980 to 1997. Ambio 28:587−591.
UNEP (1984) General Assessment of Progress in the Implementation of the Plan of Action to Combat Desertification, 1978–1984. GC-12/9 United Nations Environmental Program.
UNSO Office to Combat Desertification and Drought (1997) Aridity Zones and Dryland Populations: An Assessment of Population Levels in the World's Drylands. UNSO/UNDP, New York. 23pp.
Van Leeuwen W.J.D., Huete A.R., Laing T.W. (1999) MODIS Vegetation Index Compositing Approach - analysis and removal. Remote Sensing of Environment 69:264-280.
Xie, P. P., & Arkin, P. A. (1997) Global precipitation: A 17-year monthly analysis based on gauge observations, satellite estimates, and numerical model outputs. Bulletin of the American Meteorological Society 78:2539−2558.
Zhan X., Sohlberg R.A., Townshend J.R.G., DiMiceli C., Carroll M.L., Eastman J.C., Hansen M.C., DeFries R.S. (2002) Detection of land cover changes using MODIS 250 m data. Remote Sensing of Environment 83:336-350.
Zhang XY, Friedl MA, Schaaf CB, Strahler AH, Hodges JCF, Gao F, Reed BC, Huete A (2003) Monitoring vegetation phenology using MODIS. Remote Sensing of Environment 84: 471-475
Zhang, X., M. A. Friedl, C. B. Schaaf, A. H. Strahler, and Z. Liu (2005) Monitoring the response of vegetation phenology to precipitation in Africa by coupling MODIS and TRMM instruments. Journal of Geophysical Research 110:D12103.

Internet sources

Dryland Science for Development (DSD)
http://www.drylandscience.org, viewed 10/25/2010

Famine Early Warning Systems Network (FEWS NET)
http://www.fews.net/docs/, viewed 05/25/2011
http://earlywarning.usgs.gov/fews/africa/index.php, viewed 05/20/2011

Food and Agricultural Organization (FAO)
www.fao.org/fileadmin/templates/tc/tce/pdf/Sudan_seasonal_monitor_Nov07.pdf, viewed 05/24/2011

Joint Institute for the Study of the Atmosphere and Ocean (JISAO)
http://jisao.washington.edu/data_sets/sahel/, viewed 03/02/2011

National Aeronautics and Space Administration (NASA)
https://wist.echo.nasa.gov/api/, viewed 11/20/2010
http://modis.gsfc.nasa.gov/, viewed 09/25/2010.

http://www-modis.bu.edu/landcover/userguidelc/lc.html, viewed 02/06/2011
http://modis-250m.nascom.nasa.gov/cgi-bin/QA, viewed 01/25/2011

United States Department of Agriculture (USDA)
http://www.pecad.fas.usda.gov/, viewed 03/15/2011

Wikipedia
http://en.wikipedia.org/wiki/Phenology, viewed 03/21/2011
http://en.wikipedia.org/wiki/Geography_of_Chad, viewed 04/24/2011
http://en.wikipedia.org/wiki/Geography_of_Sudan, viewed 04/24/2011

Appendices

Appendix A

Table A1: Reclassification of MODIS land cover product (MOD12Q1)

ID	LC Reclassified	IGBP land cover type[5]	IGBP_ID
0	Water	Water	0
1	Forest	Evergreen needleleaf forest	1
		Evergreen broadleaf forest	2
		Deciduous needleleaf forest	3
		Deciduous broadleaf forest	4
		Mixed forests	5
2	Shrubland	Closed shrubland	6
		Open shrublands	7
3	Savanna	Woody Savanna	8
		Savanna	9
4	Grassland	Grassland	10
5	Wetland	Permanent wetlands	11
6	Croplands	Croplands	12
		Cropland/natural vegetation mosaic	14
7	Urban and built-up	Urban and built-up	13
8	Barren or sparsely vegetated	Barren or sparsely vegetated	16

[5] MODIS MOD12 Land Cover and Land Cover Dynamics Products User Guide
http://www-modis.bu.edu/landcover/userguidelc/lc.html

Appendix B: Sensitivity analysis to the adaptation strength parameter

B1: Large integral response to adaptation strength values of 3 and 4 in shrubland
(no seasonality is observed when adaptation strength is set to 2, and is not included).

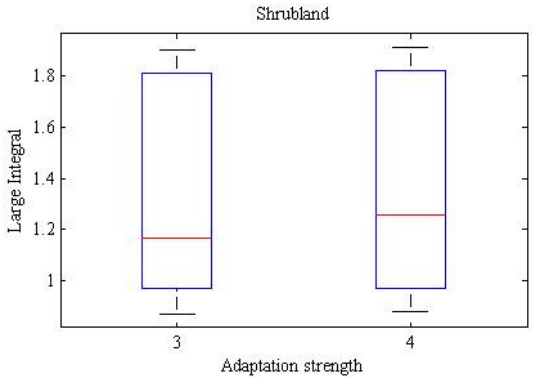

B2: Small integral (left) and season length (right) responses to adaptation strength values of 2, 3 and 4 in savanna

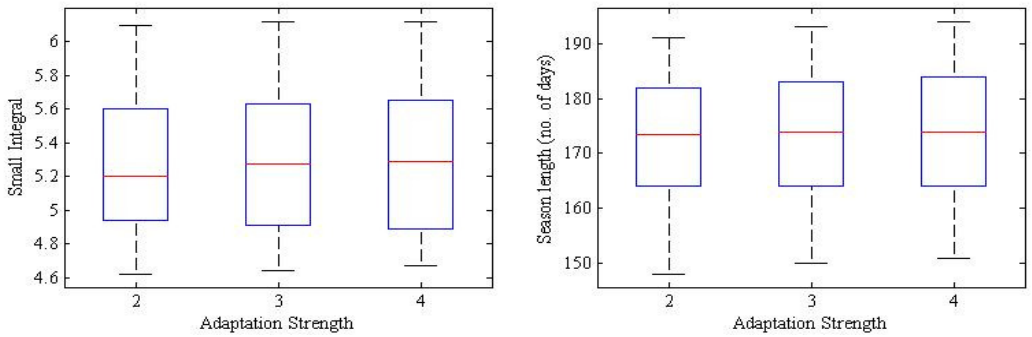

B3: Seasonal amplitude (left) and large integral (right) responses to adaptation strength values of 2, 3 and 4 in savanna

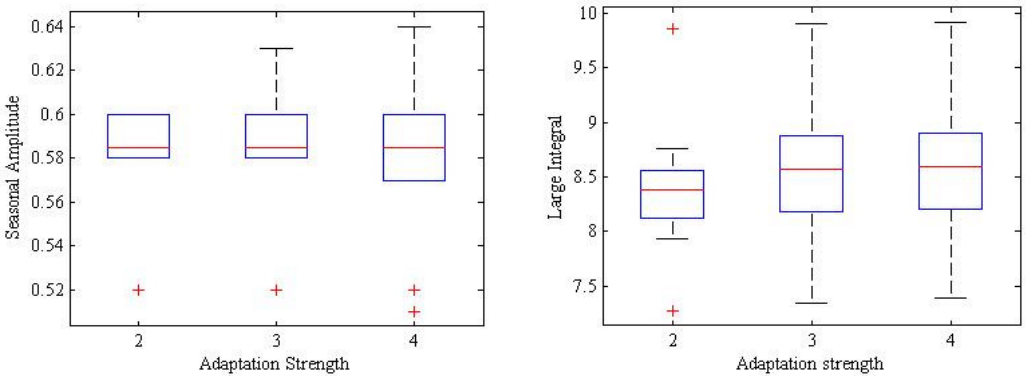

Appendix C: Seasonality parameter outputs for different land cover classes

C1: Seasonality parameters for shrubland based on Asymmetric Gaussian function

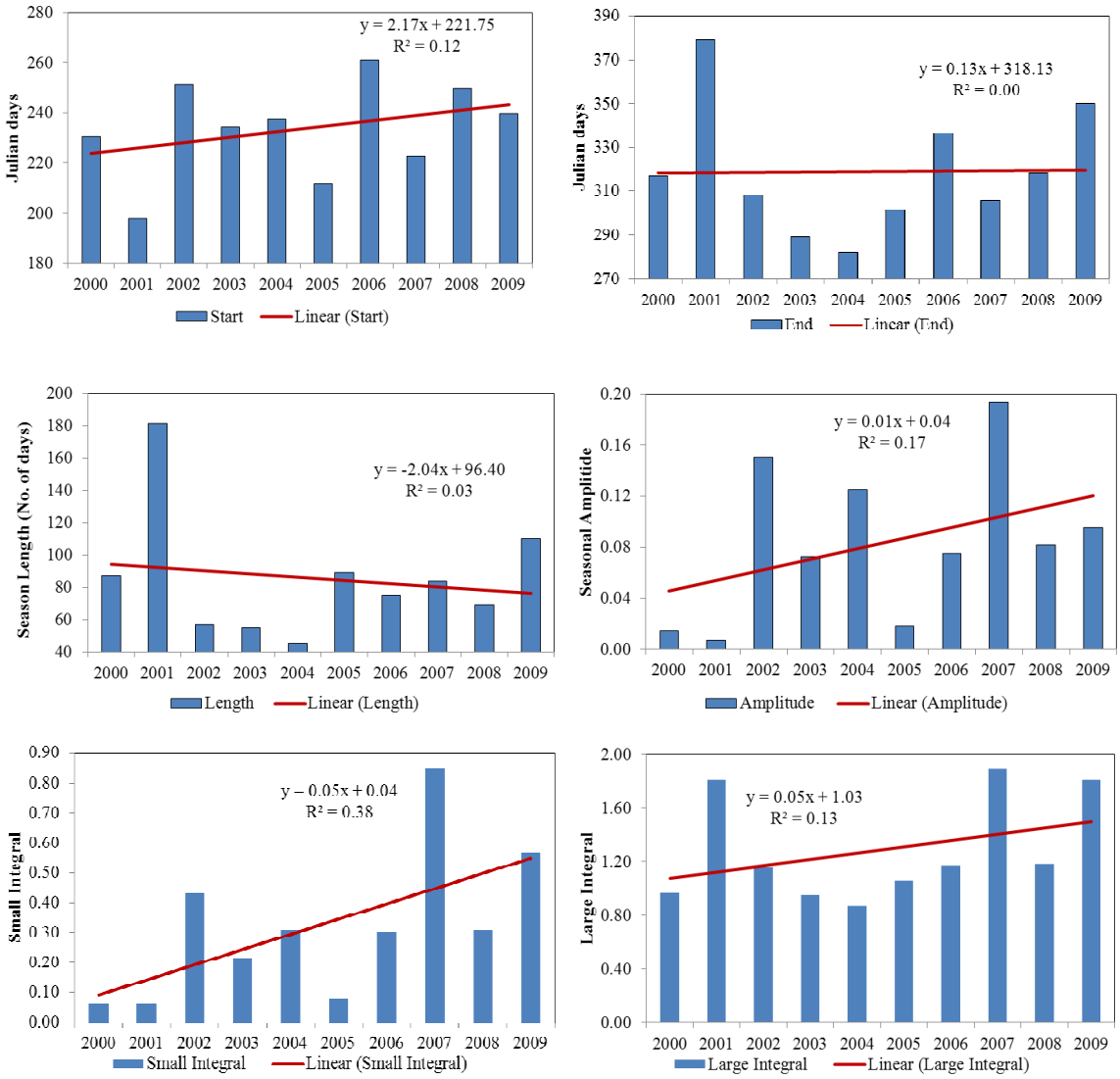

C2: Seasonality parameters for grassland (Sudan) based on adaptive Savitzky-Golay filtering

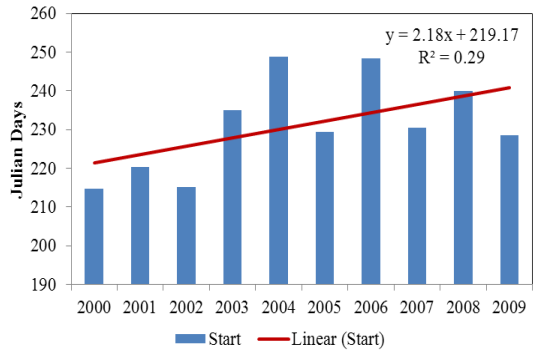

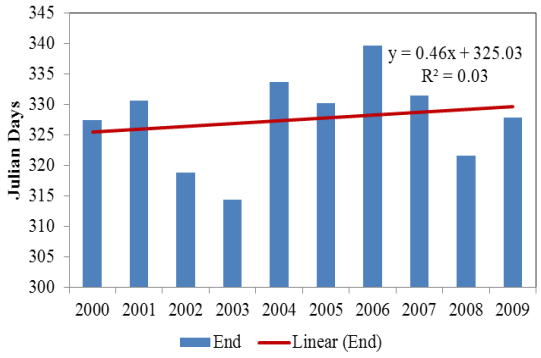

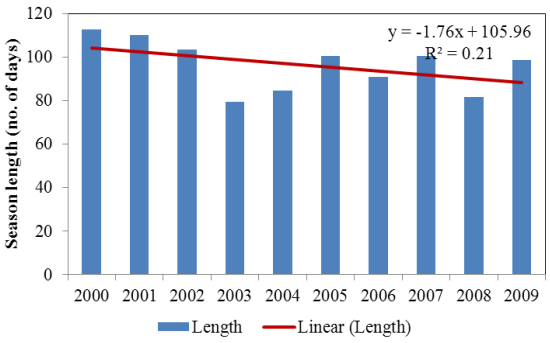

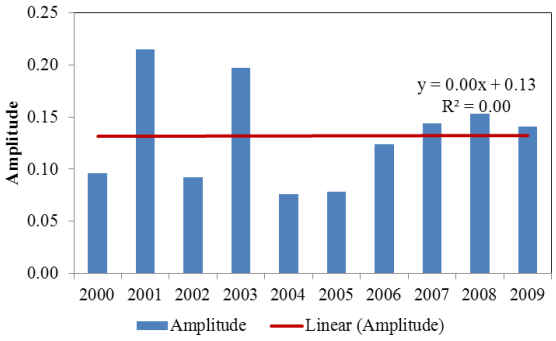

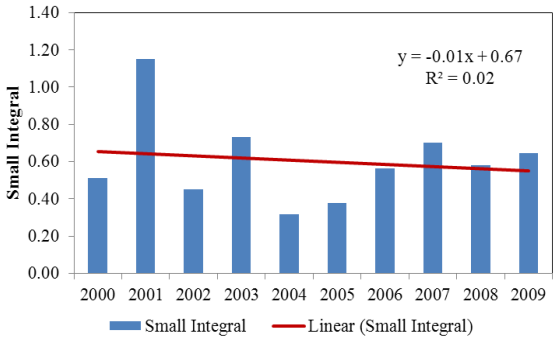

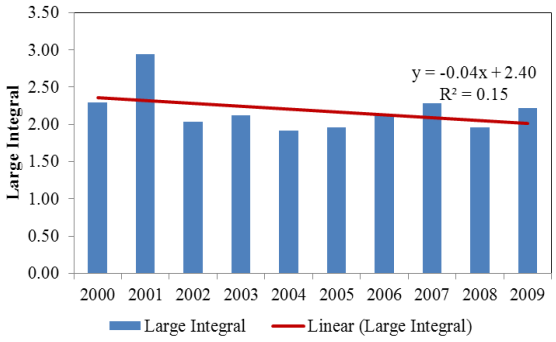

C3: Seasonality parameters for grassland (Chad) based on adaptive Savitzky-Golay filtering

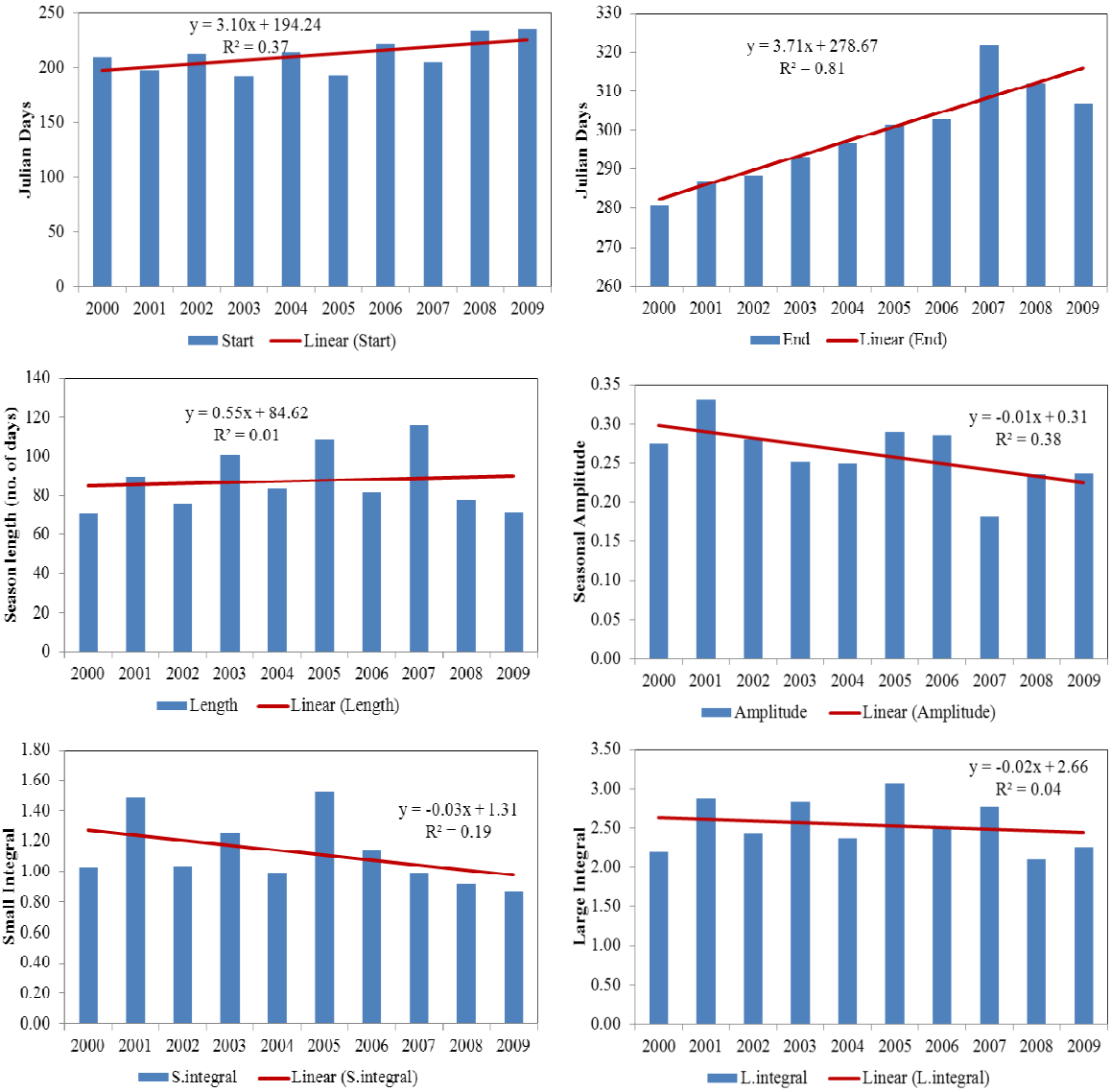

C4: Seasonality parameters for cropland based on Asymmetric Gaussian function

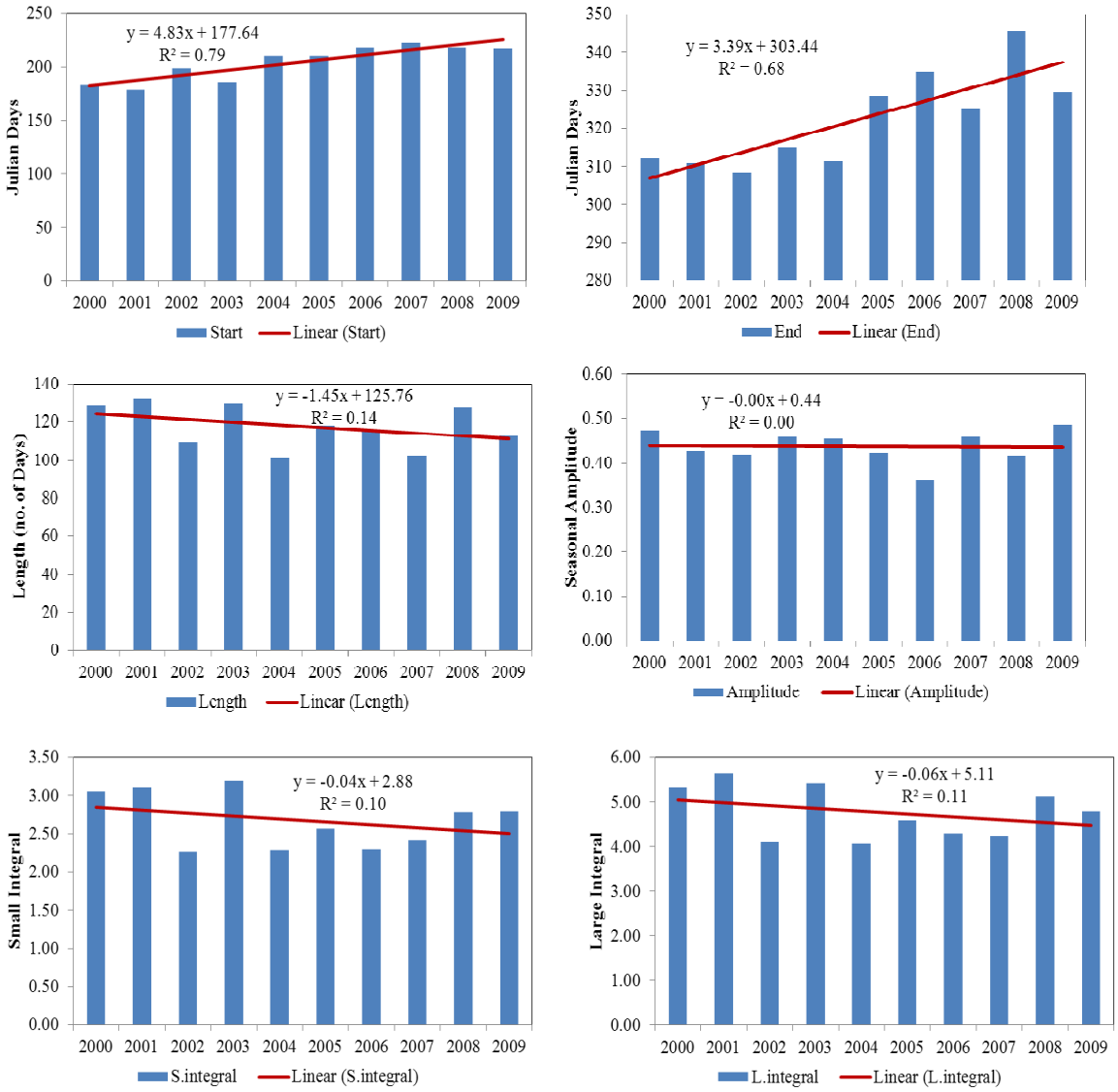

C5: Seasonality parameters for savanna based on Double Logistic function

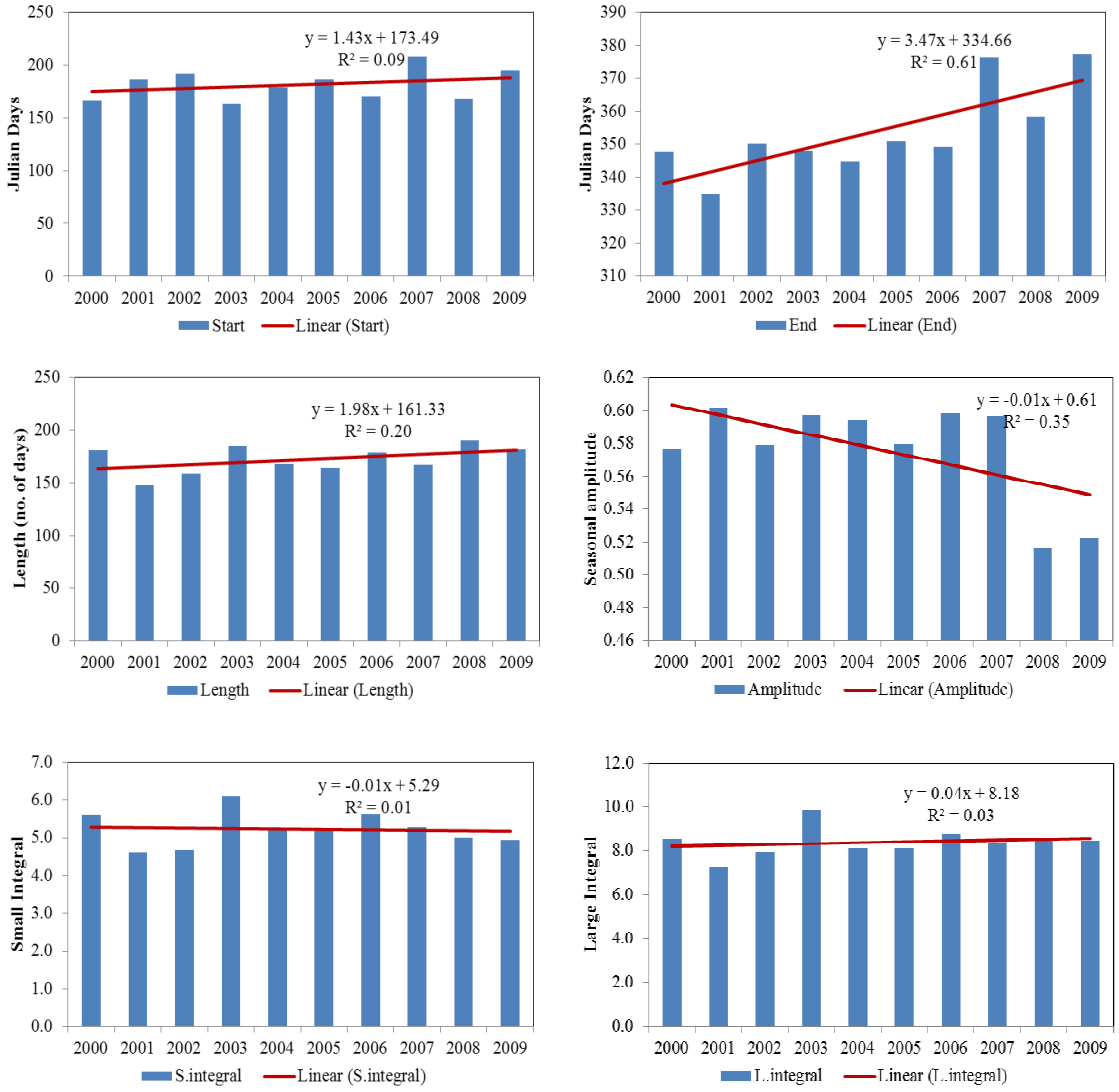

Appendix D: Statistical test outputs

Table D1: Statistical test results for NDVI, overall trend and seasonality parameters in shrubland with 95% significance level and n-2 degrees of freedom: mean1 = 2000-2004 and mean2= 2005-2009

Parameters	Mean1	Mean2	t-value	Trend	Significance
Overall trend∗	0.15	0.16	3.116	Increase	Significant
Season start	230	237	0.557	Increase	Not significant
Season end	315	322	0.360	Steady	Not significant
Season length	85	84	0.038	Decrease	Not significant
Amplitude	0.07	0.09	0.495	Increase	Not significant
Small integral	0.22	0.42	1.337	Increase	Not significant
Large integral	1.15	1.42	1.095	Increase	Not significant

∗ Mean1 = 2000-2005 and mean2 = 2006-2010

Table D2: Statistical test results for NDVI overall trend and seasonality parameters in grassland (Sudan) with 95% significance level and n-2 degrees of freedom: mean1 = 2000-2004 and mean2= 2005-2009

Parameters	Mean1	Mean2	t-value	Trend	Significance
Overall trend∗	0.23	0.22	1.708	Decrease	Not significant
Season start	227	235	1.047	Increase	Not significant
Season end	325	330	1.077	Increase	Not significant
Season length	98	94	0.516	Decrease	Not significant
Amplitude	0.14	0.13	0.312	Steady	Not significant
Small integral	0.63	0.57	0.386	Decrease	Not significant
Large integral	2.26	2.11	0.780	Decrease	Not significant

∗ Mean1 = 2000-2005 and mean2 = 2006-2010

Table D3: Statistical test results for NDVI overall trend and seasonality parameters in grassland (Chad) with 95% significance level and n-2 degrees of freedom: mean1 = 2000-2004 and mean2= 2005-2009

Parameters	Mean1	Mean2	t-value	Trend	Significance
Overall trend∗	0.25	0.24	1.039	Increase	Not significant
Season start	205	217	1.289	Increase	Not significant
Season end	289	309	4.338	Increase	Significant
Season length	84	91	0.680	Increase	Not significant
Amplitude	0.28	0.25	1.220	Decrease	Not significant
Small integral	1.16	1.09	0.464	Decrease	Not significant
Large integral	2.54	2.54	0.0	Decrease	Not significant

∗ Mean1 = 2000-2005 and mean2 = 2006-2010

Table D4: Statistical test results for NDVI overall trend and seasonality parameters in cropland with 95% significance level and n-2 degrees of freedom: mean1 = 2000-2004 and mean2= 2005-2009

Parameters	Mean1	Mean2	t-value	Trend	Significance
Overall trend*	0.37	0.36	0.488	Steady	Not significant
Season start	191	217	4.197	Increase	Significant
Season end	312	333	5.601	Increase	Significant
Season length	120	115	0.661	Decrease	Not significant
Amplitude	0.45	0.43	0.862	Steady	Not significant
Small integral	2.78	2.57	0.908	Decrease	Not significant
Large integral	4.91	4.61	0.791	Decrease	Not significant

* Mean1 = 2000-2005 and mean2 = 2006-2010

Table D5: Statistical test results for NDVI overall trend and seasonality parameters in savanna with 95% significance level and n-2 degrees of freedom: mean1 = 2000-2004 and mean2= 2005-2009

Parameters	Mean1	Mean2	t-value	Trend	Significance
Overall trend*	0.49	0.50	0.351	Increase	Not significant
Season start	177	185	0.850	Increase	Not significant
Season end	345	362	2.561	Increase	Significant
Season length	168	177	1.067	Increase	Not significant
Amplitude	0.59	0.56	1.605	Decrease	Not significant
Small integral	5.25	5.21	0.131	Decrease	Not significant
Large integral	8.35	8.43	0.181	Increase	Not significant

* Mean1 = 2000-2005 and mean2 = 2006-2010

Table D6: Statistical test results for rainfall with 95% significance level and n-2 degrees of freedom (based on the rainy season May-October) mean1 = 2001-2005 and mean2= 2006-2010..

Parameters	Mean1	Mean2	t-value	Trend	Significance
Shrubland	138.3	144.9	0.212	Decrease	Not significant
Grassland (Sudan)	259.3	310.2	1.096	Increase	Not significant
Grassland (Chad)	521.5	406.7	1.601	Decrease	Not significant
Cropland	628.9	585.6	0.554	Decrease	Not significant
Savanna	692.6	680.6	0.204	Decrease	Not significant
Barren/Sparse	17.9	22.0	0.452	Increase	Not significant

Appendix E: Comparison of amplitude between 16-day and 8-day composite images

E1: Correlation of amplitude between 16-day and 8-day composite images

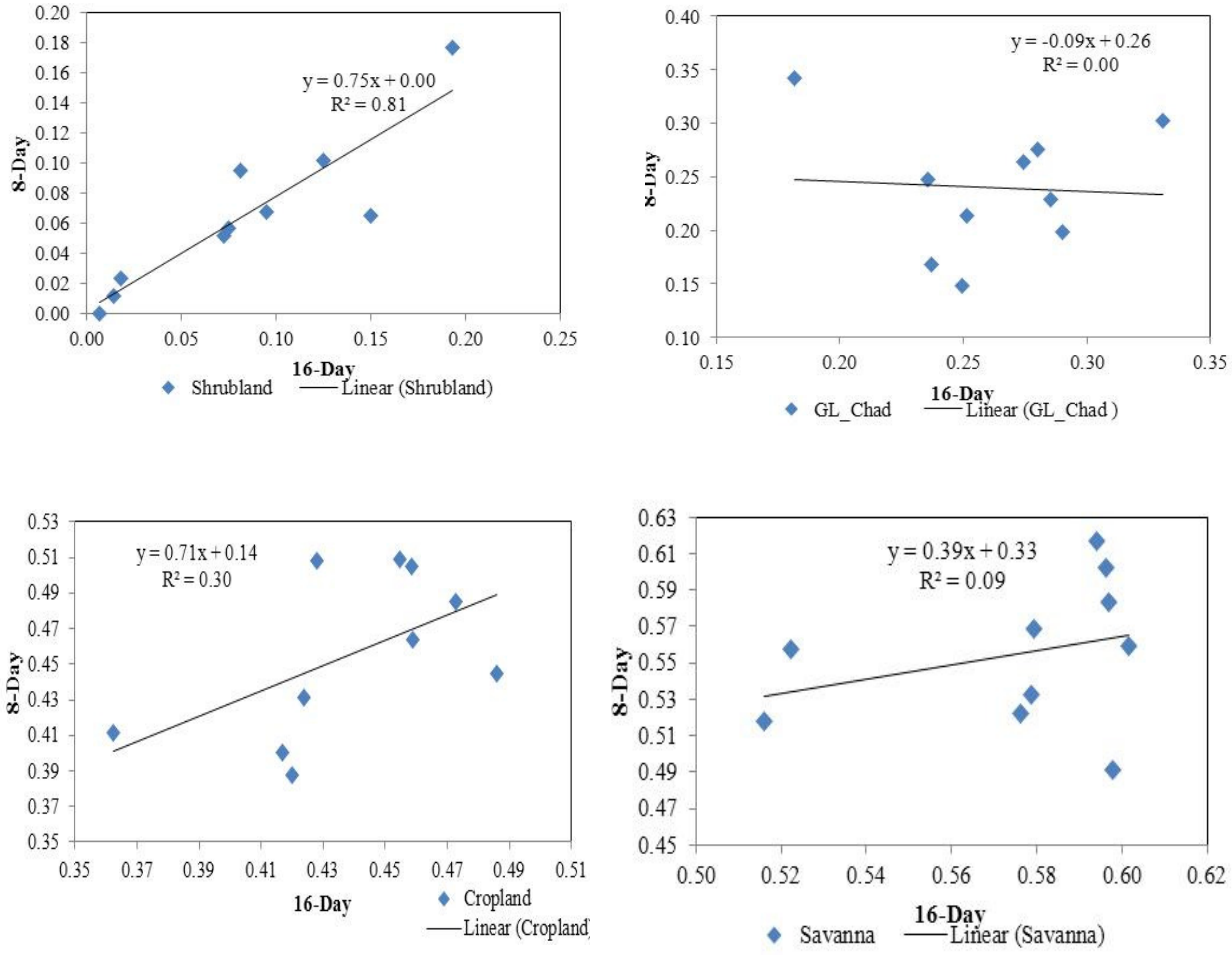

E2: Amplitude for different land cover classes 16-day (left) and 8-day (right) composite images

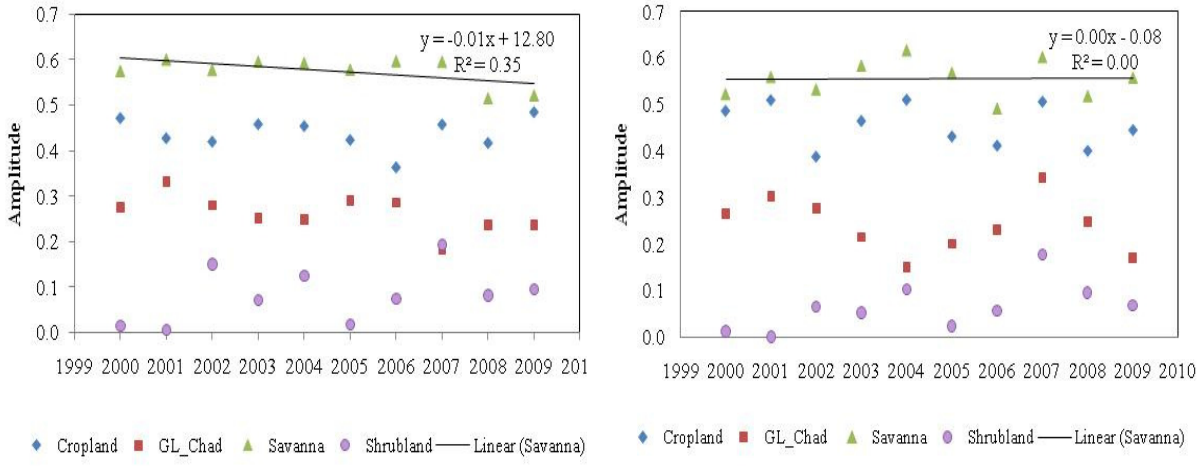

Lunds Universitets Naturgeografiska institution. Seminarieuppsatser. Uppsatserna finns tillgängliga på Naturgeografiska institutionens bibliotek, Sölvegatan 12, 223 62 LUND. Serien startade 1985. Hela listan och själva uppsatserna är även tillgängliga på http://www.geobib.lu.se/

The reports are available at the Geo-Library, Department of Physical Geography, University of Lund, Sölvegatan 12, S-223 62 Lund, Sweden.
Report series started 1985. The whole complete list and electronic versions are available at http://www.geobib.lu.se/

157 Öberg, Hanna (2009): GIS-användning i katastrofdrabbade utvecklingsländer
158 Marion Früchtl &Miriam Hurkuck (2009): Reproduction of methane emissions from terrestrial plants under aerobic conditions
159 Florian Sallaba (2009): Potential of a Post-Classification Change Detection Analysis to Identify Land Use and Land Cover Changes. A Case Study in Northern Greece
160 Sara Odelius (2009): Analys av stadsluftens kvalitet med hjälp av geografiska informationssystem.
161 Carl Bergman (2009): En undersökning av samband mellan förändringar i fenologi och temperatur 1982-2005 med hjälp av GIMMS datasetet och klimatdata från SMHI.
162 Per Ola Olsson (2009): Digitala höjdmodeller och höjdsystem. Insamling av höjddata med fokus på flygburen laserskanning.
163 Johanna Engström (2009): Landskapets påverkan på vinden -sett ur ett vindkraftperspektiv.
164 Andrea Johansson (2009): Olika våtmarkstypers påverkan på CH_4, N_2O och CO_2 utsläpp, och upptag av N_2.
165 Linn Elmlund (2009): The Threat of Climate Change to Coral Reefs
166 Hanna Forssman (2009): Avsmältningen av isen på Arktis - mätmetoder, orsaker och effekter.
167 Julia Olsson (2009): Alpina trädgränsens förändring i Jämtlands- och Dalarnas län över 100 år.
168 Helen Thorstensson (2009): Relating soil properties to biomass consumption and land management in semiarid Sudan – A Minor Field Study in North Kordofan
169 Nina Cerić och Sanna Elgh Dalgren (2009): Kustöversvämningar och GIS - en studie om Skånska kustnära kommuners arbete samt interpolations-metodens betydelse av höjddata vid översvämningssimulering.
170 Mats Carlsson (2009): Aerosolers påverkan på klimatet.
171 Elise Palm (2009): Övervakning av gåsbete av vass – en metodutveckling
172 Sophie Rychlik (2009): Relating interannual variability of atmospheric CH_4 growth rate to large-scale CH_4 emissions from northern wetlands
173 Per-Olof Seiron and Hanna Friman (2009): The Effects of Climate Induced Sea Level Rise on the Coastal Areas in the Hambantota District, Sri Lanka - A geographical study of Hambantota and an identification of vulnerable ecosystems and land use along the coast.
174 Norbert Pirk (2009): Methane Emission Peaks from Permafrost Environments:

Using Ultra–Wideband Spectroscopy, Sub-Surface Pressure Sensing and Finite Element Solving as Means of their Exploration

175 Hongxiao Jin (2010): Drivers of Global Wildfires — Statistical analyses

176 Emma Cederlund (2010): Dalby Söderskog – Den historiska utvecklingen

177 Lina Glad (2010): En förändringsstudie av Ivösjöns strandlinje

178 Erika Filppa (2010): Utsläpp till luft från ballastproduktionen år 2008

179 Karolina Jacobsson (2010):Havsisens avsmältning i Arktis och dess effekter

180 Mattias Spångmyr (2010): Global of effects of albedo change due to urbanization

181 Emmelie Johansson & Towe Andersson (2010): Ekologiskt jordbruk - ett sätt att minska övergödningen och bevara den biologiska mångfalden?

182 Åsa Cornander (2010): Stigande havsnivåer och dess effect på känsligt belägna bosättningar

183 Linda Adamsson (2010): Landskapsekologisk undersökning av ädellövskogen i Östra Vätterbranterna

184 Ylva Persson (2010): Markfuktighetens påverkan på granens tillväxt i Guvarp

185 Boel Hedgren (2010): Den arktiska permafrostens degradering och metangasutsläpp

186 Joakim Lindblad & Johan Lindenbaum (2010): GIS-baserad kartläggning av sambandet mellan pesticidförekomster i grundvatten och markegenskaper

187 Oscar Dagerskog (2010): Baösberggrottan – Historiska tillbakablickar och en lokalklimatologisk undersökning

188 Mikael Månsson (2010): Webbaserad GIS-klient för hantering av geologisk information

189 Lina Eklund (2010): Accessibility to health services in the West Bank, occupied Palestinian Territory.

190 Edvin Eriksson (2010): Kvalitet och osäkerhet i geografisk analys - En studie om kvalitetsaspekter med fokus på osäkerhetsanalys av rumslig prognosmodell för trafikolyckor

191 Elsa Tessaire (2010): Impacts of stressful weather events on forest ecosystems in south Sweden.

192 Xuejing Lei (2010): Assessment of Climate Change Impacts on Cork Oak in Western Mediterranean Regions: A Comparative Analysis of Extreme Indices

193 Radoslaw Guzinski (2010): Comparison of vegetation indices to determine their accuracy in predicting spring phenology of Swedish ecosystems

194 Yasar Arfat (2010): Land Use / Land Cover Change Detection and Quantification — A Case study in Eastern Sudan

195 Ling Bai (2010): Comparison and Validation of Five Global Land Cover Products Over African Continent

196 Raunaq Jahan (2010): Vegetation indices, FAPAR and spatial seasonality analysis of crops in southern Sweden

197 Masoumeh Ghadiri (2010): Potential of Hyperion imagery for simulation of MODIS NDVI and AVHRR-consistent NDVI time series in a semi-arid region

198 Maoela A. Malebajoa (2010): Climate change impacts on crop yields and adaptive measures for agricultural sector in the lowlands of Lesotho

199 Herbert Mbufong Njuabe (2011): Subarctic Peatlands in a Changing Climate:

Greenhouse gas response to experimentally increased snow cover

200 Naemi Gunlycke & Anja Tuomaala (2011): Detecting forest degradation in Marakwet district, Kenya, using remote sensing and GIS

201 Nzung Seraphine Ebang (2011): How was the carbon balance of Europe affected by the summer 2003 heat wave? A study based on the use of a Dynamic Global Vegetation Model; LPJ-GUESS

202 Per-Ola Olsson (2011): Cartography in Internet-based view services – methods to improve cartography when geographic data from several sources are combined

203 Kristoffer Mattisson (2011): Modelling noise exposure from roads – a case study in Burlövs municipality

204 Erik Ahlberg (2011): BVOC emissions from a subarctic Mountain birch: Analysis of short-term chamber measurements.

205 Wilbert Timiza (2011): Climate variability and satellite – observed vegetation responses in Tanzania.

206 Louise Svensson (2011): The ethanol industry - impact on land use and biodiversity. A case study of São Paulo State in Brazil.

207 Fredrik Fredén (2011): Impacts of dams on lowland agriculture in the Mekong river catchment.

208 Johanna Hjärpe (2011): Kartläggning av kväve i vatten i LKAB:s verksamhet i Malmberget år 2011 och kvävets betydelse i akvatiska ekosystem ur ett lokalt och ett globalt perspektiv.

209 Oskar Löfgren (2011): Increase of tree abundance between 1960 and 2009 in the treeline of Luongastunturi in the northern Swedish Scandes

210 Izabella Rosengren (2011): Land degradation in the Ovitoto region of Namibia: what are the local causes and consequences and how do we avoid them?

211 Irina Popova (2011): Agroforestry och dess påverkan på den biofysiska miljön i Afrika.

212 Emilie Walsund (2011): Food Security and Food Sufficiency in Ethiopia and Eastern Africa.

213 Martin Bernhardson (2011): Jökulhlaups: Their Associated Landforms and Landscape Impacts.

214 Michel Tholin (2011): Weather induced variations in raptor migration; A study of raptor migration during one autumn season in Kazbegi, Georgia, 2010

215 Amelie Lindgren (2011) The Effect of Natural Disturbances on the Carbon Balance of Boreal Forests.

216 Klara Århem (2011): Environmental consequences of the palm oil industry in Malaysia.

217 Ana Maria Yáñez Serrano (2011) Within-Canopy Sesquiterpene Ozonolysis in Amazonia

218 Edward Kashava Kuliwoye (2011) Flood Hazard Assessment by means of Remote Sensing and Spatial analyses in the Cuvelai Basin Case Study Ohangwena Region –Northern Namibia

219 Julia Olsson (2011) GIS-baserad metod för etablering av centraliserade biogasanläggningar baserad på husdjursgödsel.

220 Florian Sallaba (2011) The potential of support vector machine classification of land use and land cover using seasonality from MODIS satellite data

221 Salem Beyene Ghezahai (2011) Assessing vegetation changes for parts of the Sudan and Chad during 2000-2010 using time series analysis of MODIS-NDVI

222 Bahzad Khaled (2011) Spatial heterogeneity of soil CO2 efflux at ADVEX site Norunda in Sweden